ulm university universität uulm

Stochastic microstructure modeling of particle-based materials in 3D and 4D

Volker Schmidt
Ulm University, Institute of Stochastics

September 2016

Introduction

Compressed graphite electrodes

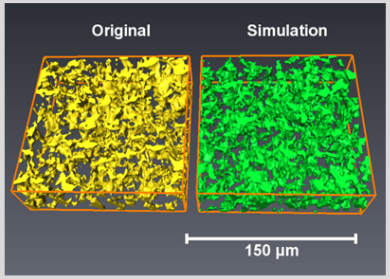

Uncompressed graphite electrodes

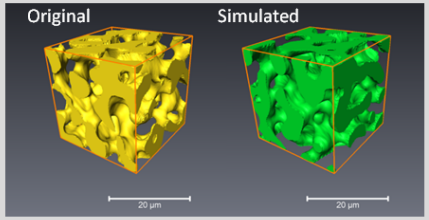

Hybrid organic solar cells

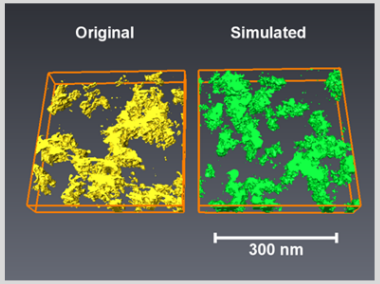

SOFC cathodes

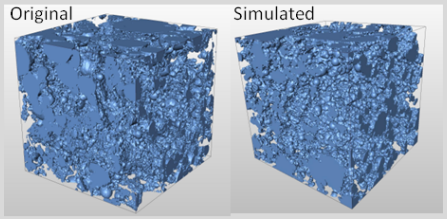

Ulm University
Institute of Stochastics

Molecular networks

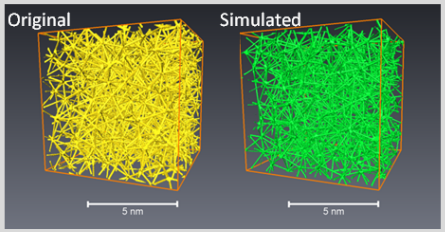

Eutetic Si corals in Al-Si alloys

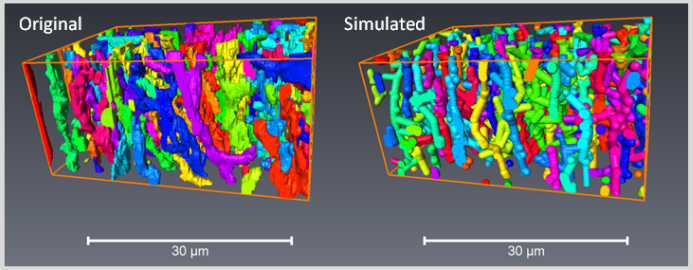

Non-woven GDL

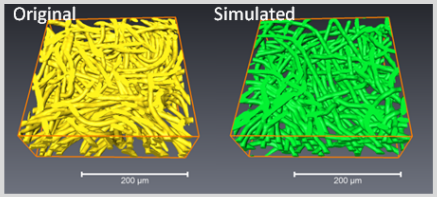

Stochastic microstructure modeling

Impact of the microstructure

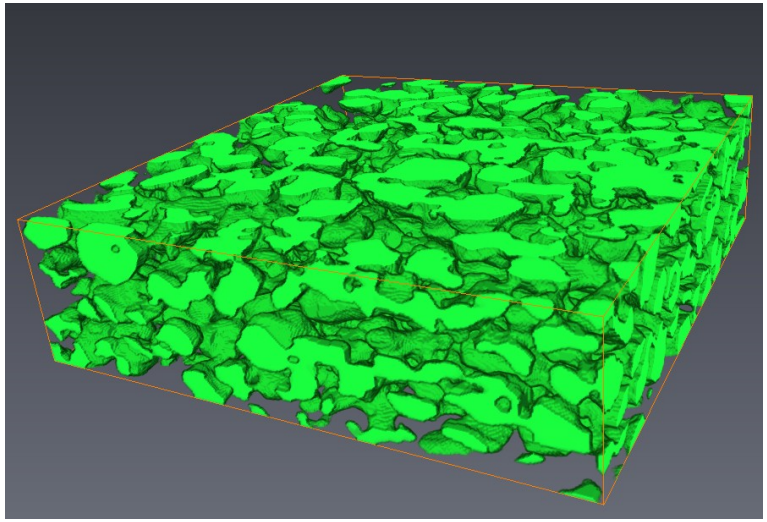

Stochastic microstructure modeling

Impact of the microstructure

- morphology of anodes influences electrochemical performance

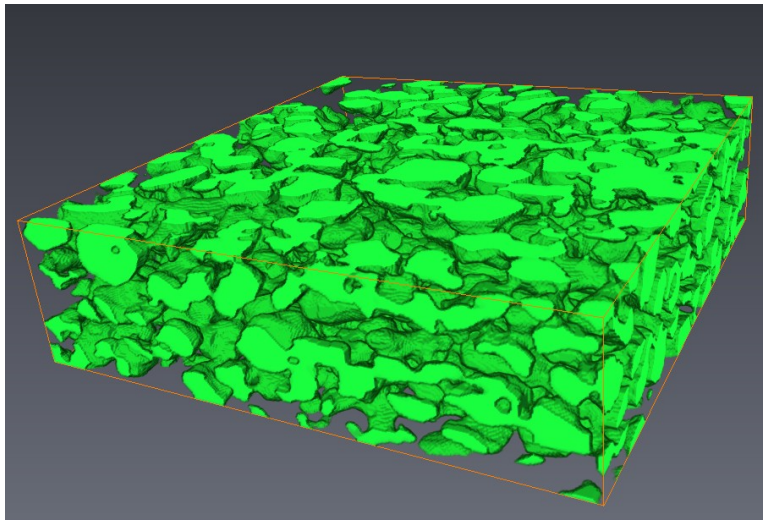

Stochastic microstructure modeling

Impact of the microstructure

- morphology of anodes influences electrochemical performance
  - capacity and power

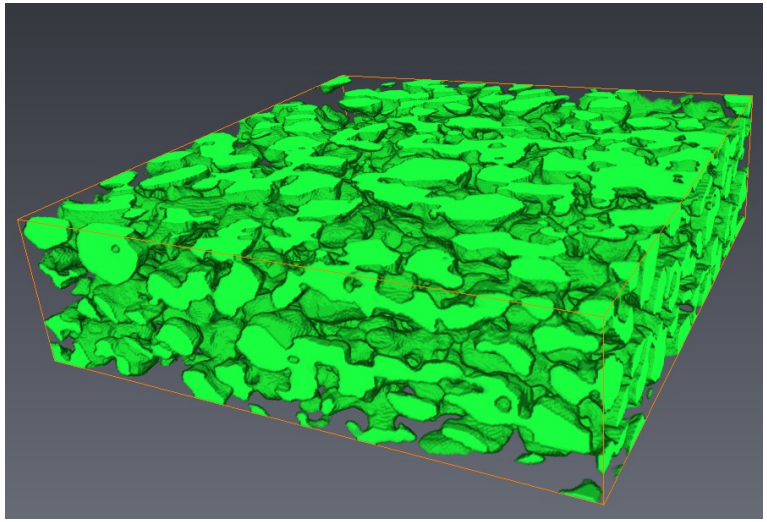

Stochastic microstructure modeling

Impact of the microstructure

- morphology of anodes influences electrochemical performance
  - capacity and power
  - degradation and aging

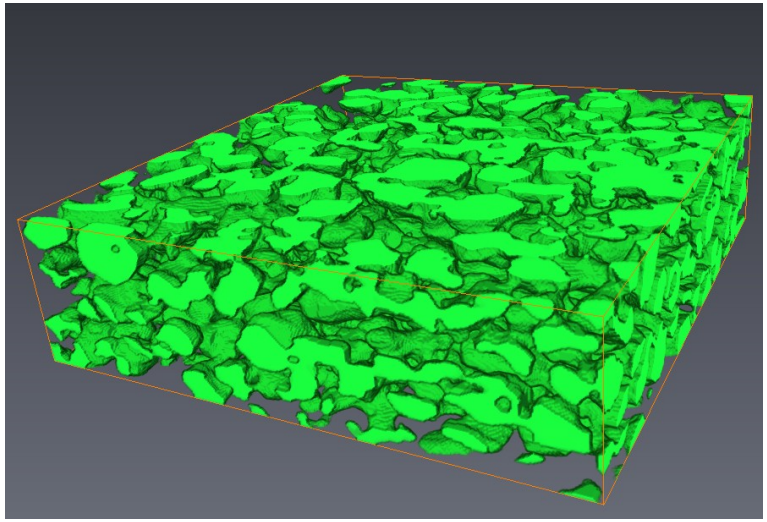

Stochastic microstructure modeling

Impact of the microstructure

- morphology of anodes influences electrochemical performance
  - capacity and power
  - degradation and aging

Laboratory experiments

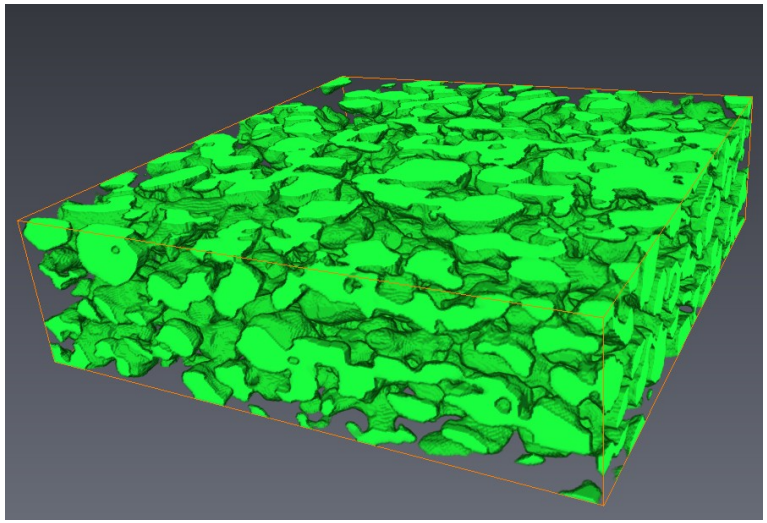

Stochastic microstructure modeling

Impact of the microstructure

- morphology of anodes influences electrochemical performance
  - capacity and power
  - degradation and aging

Laboratory experiments

- expensive in cost and time

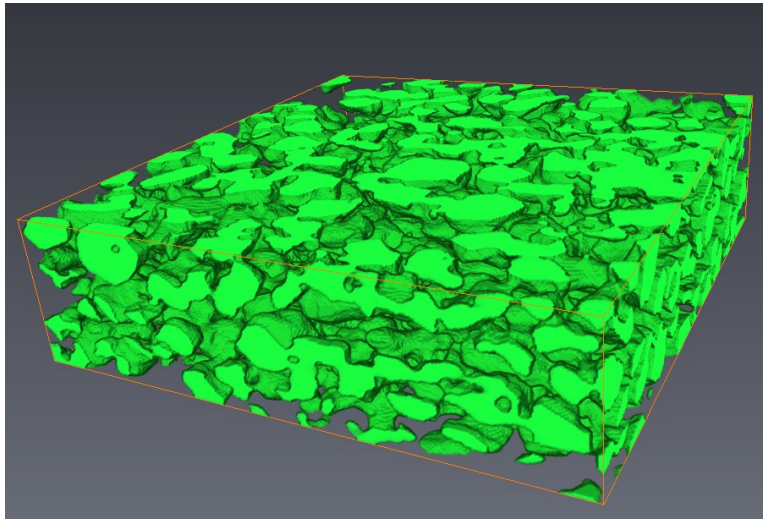

Stochastic microstructure modeling

Impact of the microstructure

- morphology of anodes influences electrochemical performance
  - capacity and power
  - degradation and aging

Laboratory experiments

- expensive in cost and time
- information about
  - impact of processing parameters

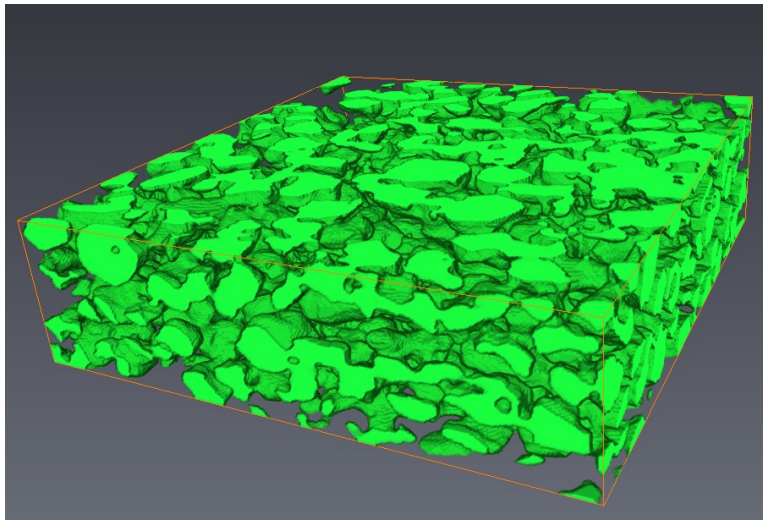

Stochastic microstructure modeling

Impact of the microstructure

- morphology of anodes influences electrochemical performance
  - capacity and power
  - degradation and aging

Laboratory experiments

- expensive in cost and time
- information about
  - impact of processing parameters
  - but not of microstructure

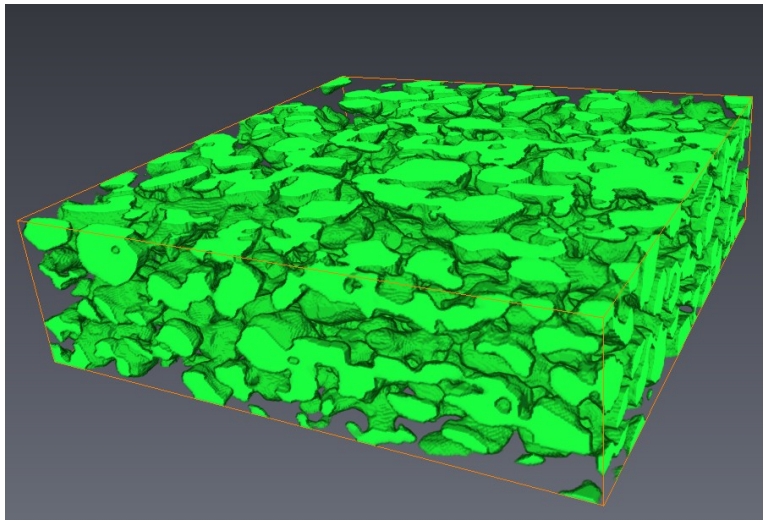

Stochastic microstructure modeling

Impact of the microstructure

- morphology of anodes influences electrochemical performance
  - capacity and power
  - degradation and aging

Laboratory experiments

- expensive in cost and time
- information about
  - impact of processing parameters
  - but not of microstructure

Goal

- cost- and time-efficient method to find morphologies with optimized functionality

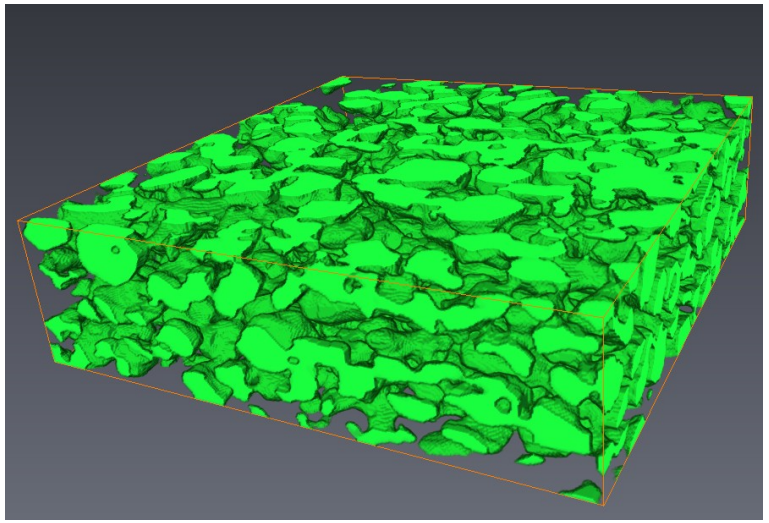

Stochastic microstructure modeling

Impact of the microstructure

- morphology of anodes influences electrochemical performance
  - capacity and power
  - degradation and aging

Laboratory experiments

- expensive in cost and time
- information about
  - impact of processing parameters
  - but not of microstructure

Goal

- cost- and time-efficient method to find morphologies with optimized functionality

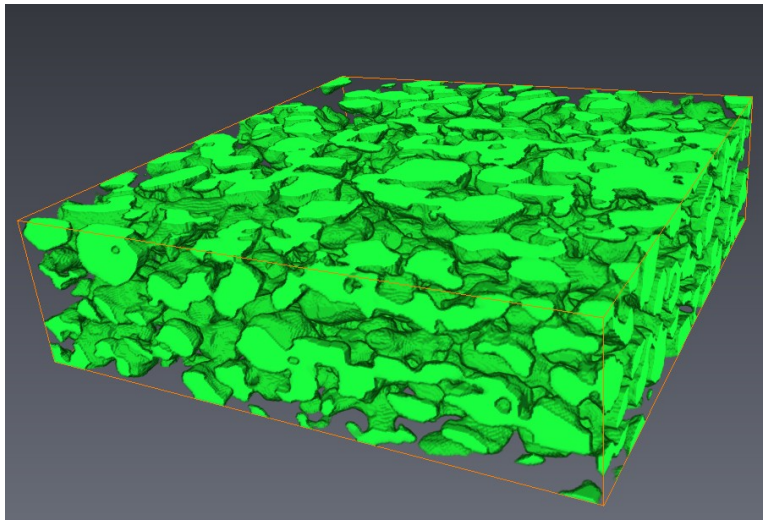

Approach via stochastic modeling

Stochastic microstructure modeling

Impact of the microstructure

- morphology of anodes influences electrochemical performance
  - capacity and power
  - degradation and aging

Laboratory experiments

- expensive in cost and time
- information about
  - impact of processing parameters
  - but not of microstructure

Goal

- cost- and time-efficient method to find morphologies with optimized functionality

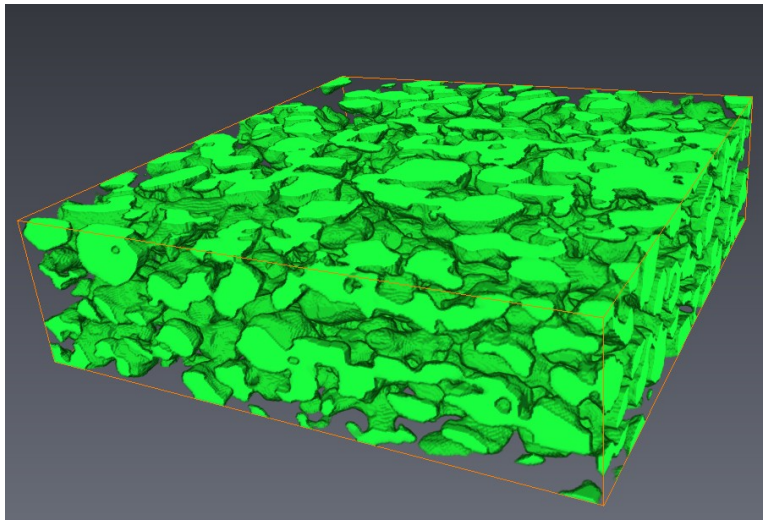

Approach via stochastic modeling

- fit parametric microstructure model to experimental data

Stochastic microstructure modeling

Impact of the microstructure

- morphology of anodes influences electrochemical performance
  - capacity and power
  - degradation and aging

Laboratory experiments

- expensive in cost and time
- information about
  - impact of processing parameters
  - but not of microstructure

Goal

- cost- and time-efficient method to find morphologies with optimized functionality

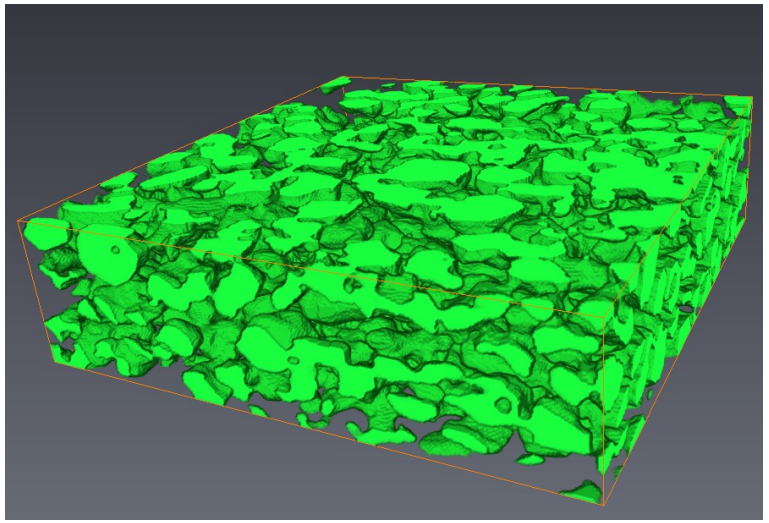

Approach via stochastic modeling

- fit parametric microstructure model to experimental data
- generate virtual morphologies

Stochastic microstructure modeling

Impact of the microstructure

- morphology of anodes influences electrochemical performance
  - capacity and power
  - degradation and aging

Laboratory experiments

- expensive in cost and time
- information about
  - impact of processing parameters
  - but not of microstructure

Goal

- cost- and time-efficient method to find morphologies with optimized functionality

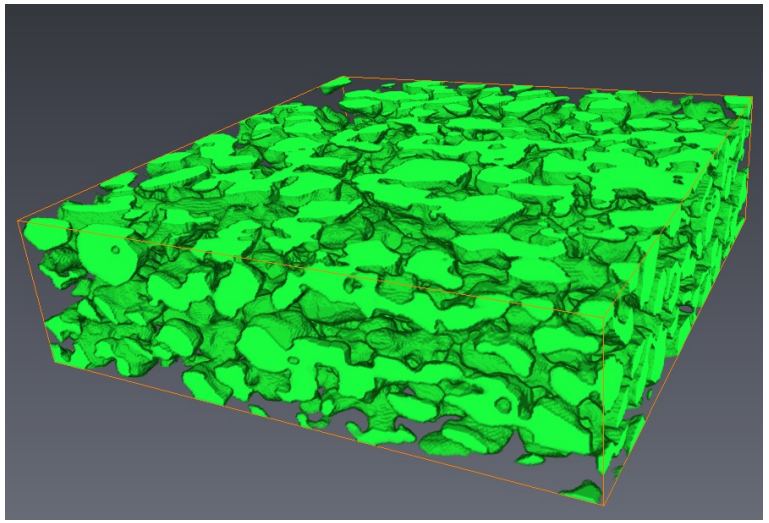

Approach via stochastic modeling

- fit parametric microstructure model to experimental data
- generate virtual morphologies
- virtual materials testing via spatially resolved transport models

Stochastic microstructure modeling

Impact of the microstructure

- morphology of anodes influences electrochemical performance
  - capacity and power
  - degradation and aging

Laboratory experiments

- expensive in cost and time
- information about
  - impact of processing parameters
  - but not of microstructure

Goal

- cost- and time-efficient method to find morphologies with optimized functionality

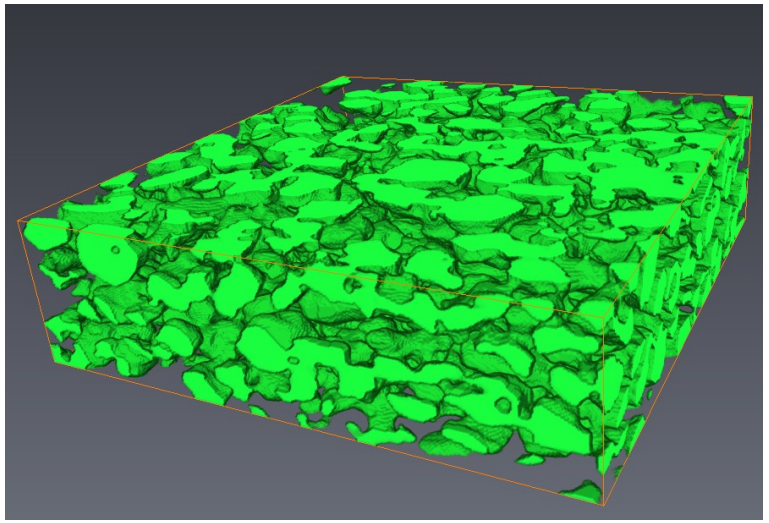

Approach via stochastic modeling

- fit parametric microstructure model to experimental data
- generate virtual morphologies
- virtual materials testing via spatially resolved transport models
- identify preferable morphologies

Parametric representation of particles

J. Feinauer, A. Spettl, I. Manke, S. Strege, A. Kwade, A. Pott and V. Schmidt, Structural characterization of particle systems using spherical harmonics. *Materials Characterization* 106 (2015), 123-133.

Parametric representation of particles

Spherical harmonics

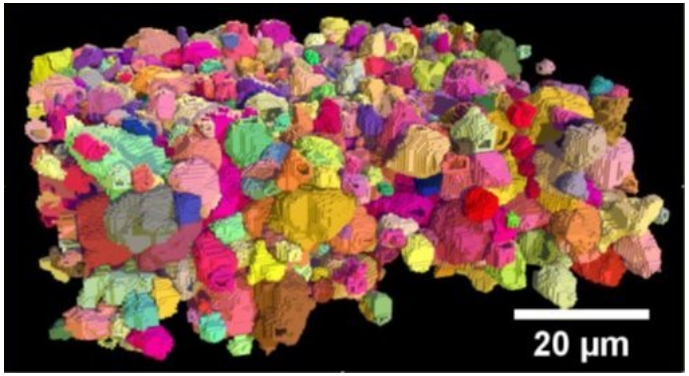

J. Feinauer, A. Spettl, I. Manke, S. Strege, A. Kwade, A. Pott and V. Schmidt, Structural characterization of particle systems using spherical harmonics. *Materials Characterization* 106 (2015), 123-133.

Parametric representation of particles

Spherical harmonics

- represent particles as radius function depending on two angles

$$r(\theta,\phi) = \sum_{l=0}^{\infty} \sum_{m=-l}^{l} c_l^m Y_l^m(\theta,\phi),$$

$c_l^m \rightarrow$ spherical harmonic coefficients

$Y_l^m \rightarrow$ spherical harmonic functions

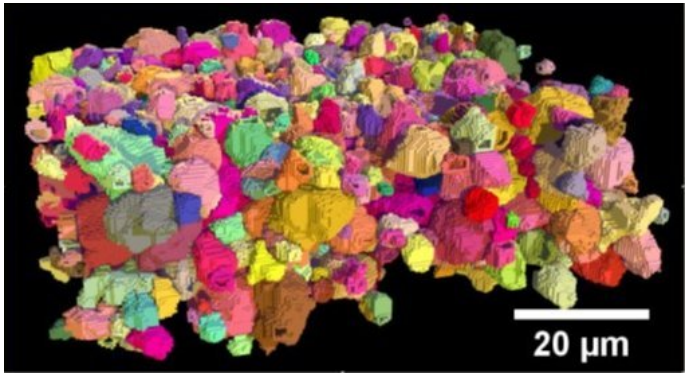

J. Feinauer, A. Spettl, I. Manke, S. Strege, A. Kwade, A. Pott and V. Schmidt, Structural characterization of particle systems using spherical harmonics. *Materials Characterization* 106 (2015), 123-133.

Parametric representation of particles

Spherical harmonics

- represent particles as radius function depending on two angles

$$r(\theta,\phi) = \sum_{l=0}^{L} \sum_{m=-l}^{l} c_l^m Y_l^m(\theta,\phi),$$

$c_l^m \rightarrow$ spherical harmonic coefficients

$Y_l^m \rightarrow$ spherical harmonic functions

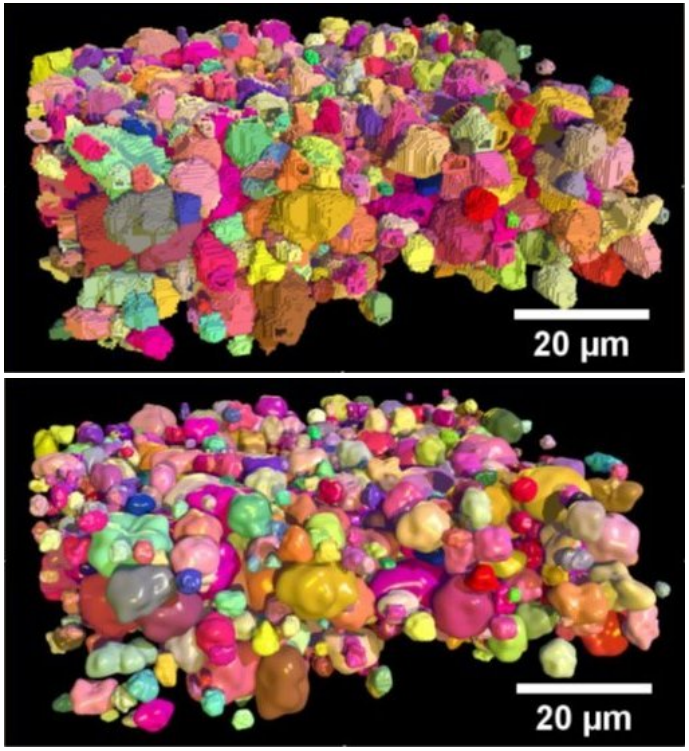

J. Feinauer, A. Spettl, I. Manke, S. Strege, A. Kwade, A. Pott and V. Schmidt, Structural characterization of particle systems using spherical harmonics. *Materials Characterization* 106 (2015), 123-133.

Parametric representation of particles

Spherical harmonics

- represent particles as radius function depending on two angles

$$r(\theta,\phi) = \sum_{l=0}^{L} \sum_{m=-l}^{l} c_l^m Y_l^m(\theta,\phi),$$

$c_l^m \rightarrow$ spherical harmonic coefficients

$Y_l^m \rightarrow$ spherical harmonic functions

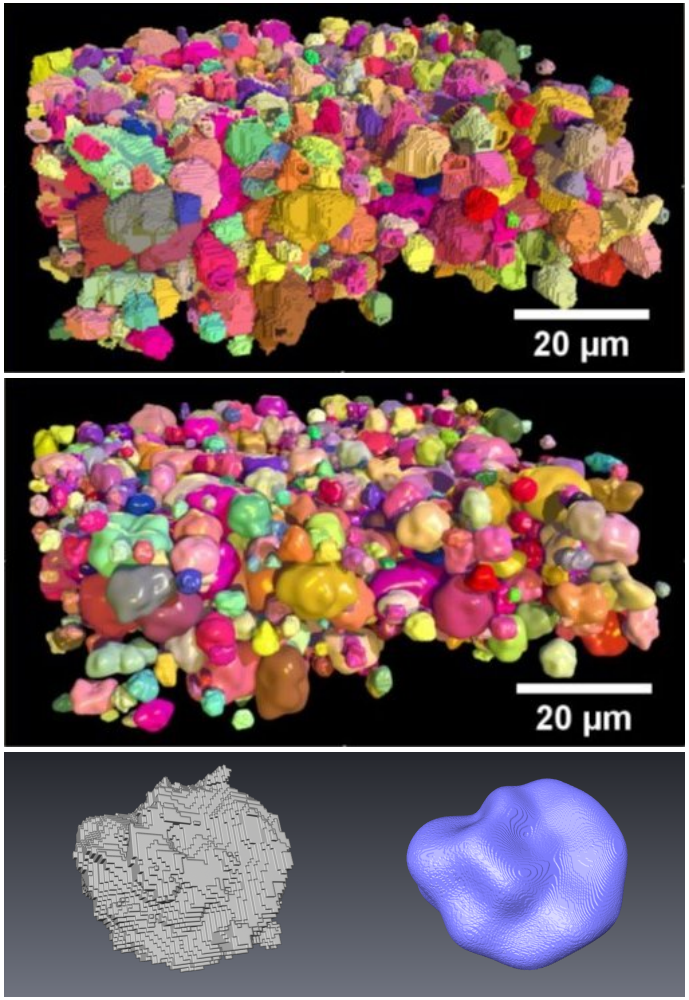

J. Feinauer, A. Spettl, I. Manke, S. Strege, A. Kwade, A. Pott and V. Schmidt, Structural characterization of particle systems using spherical harmonics. *Materials Characterization* 106 (2015), 123-133.

Parametric representation of particles

Spherical harmonics

- represent particles as radius function depending on two angles

$$r(\theta,\phi) = \sum_{l=0}^{L} \sum_{m=-l}^{l} c_l^m Y_l^m(\theta,\phi),$$

$c_l^m \rightarrow$ spherical harmonic coefficients

$Y_l^m \rightarrow$ spherical harmonic functions

- fit multivariate normal distribution to coefficients c_l^m

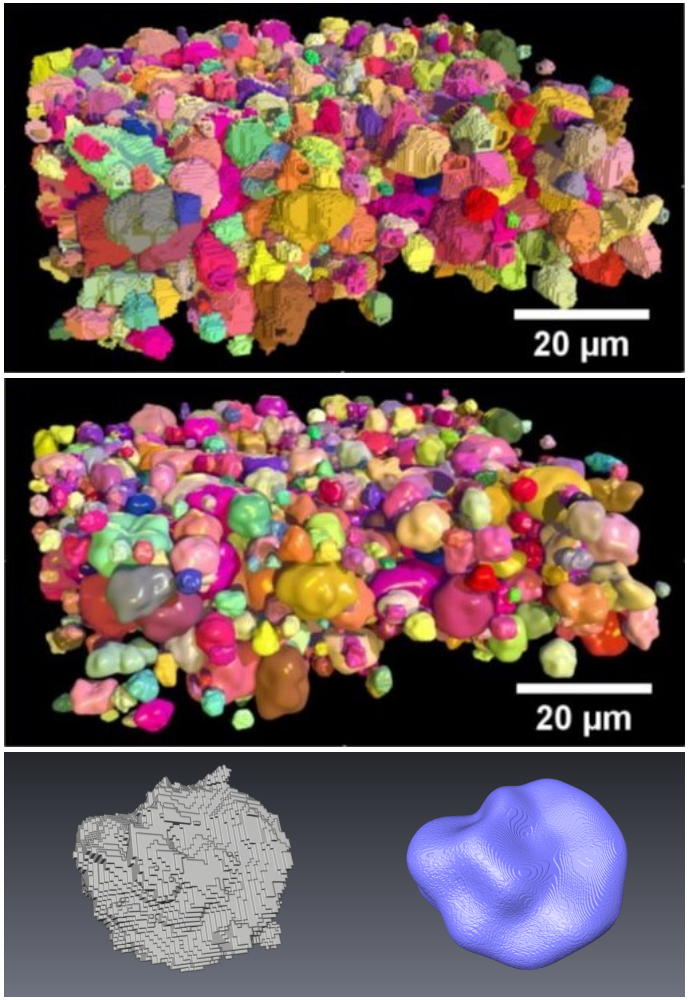

J. Feinauer, A. Spettl, I. Manke, S. Strege, A. Kwade, A. Pott and V. Schmidt, Structural characterization of particle systems using spherical harmonics. *Materials Characterization* 106 (2015), 123-133.

Parametric representation of particles

Spherical harmonics

- represent particles as radius function depending on two angles

$$r(\theta,\phi) = \sum_{l=0}^{L} \sum_{m=-l}^{l} c_l^m Y_l^m(\theta,\phi),$$

$c_l^m \rightarrow$ spherical harmonic coefficients

$Y_l^m \rightarrow$ spherical harmonic functions

- fit multivariate normal distribution to coefficients c_l^m
- sample from this distribution

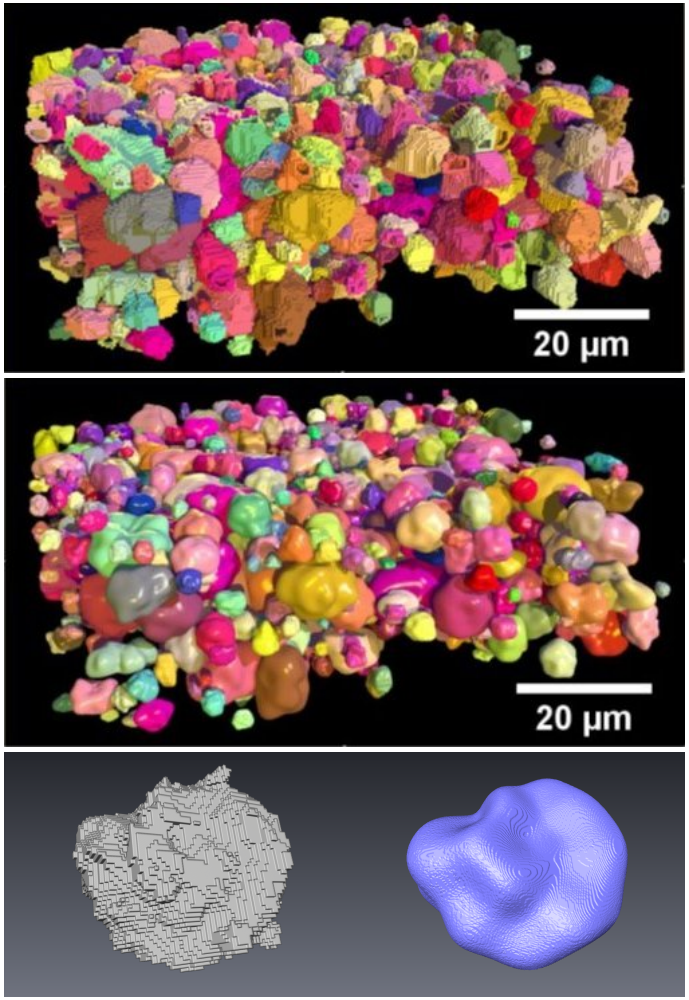

J. Feinauer, A. Spettl, I. Manke, S. Strege, A. Kwade, A. Pott and V. Schmidt, Structural characterization of particle systems using spherical harmonics. *Materials Characterization* 106 (2015), 123-133.

Anodes of energy cells

J. Feinauer, T. Brereton, A. Spettl, M. Weber, I. Manke and V. Schmidt, Stochastic 3D modeling of the microstructure of lithium-ion battery anodes via Gaussian random fields on the sphere. *Computational Materials Science* 109 (2015), 137-146.

Anodes of energy cells

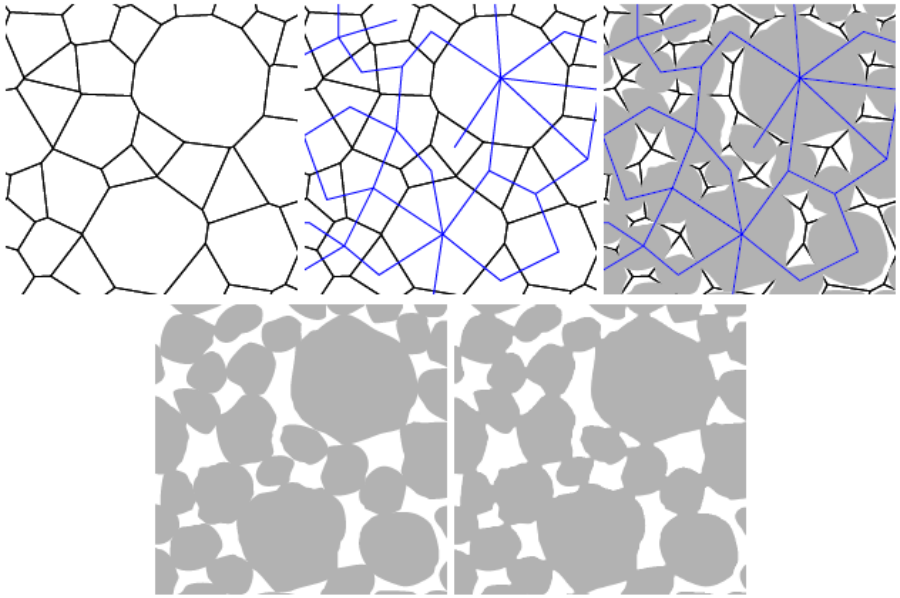

Modeling idea

J. Feinauer, T. Brereton, A. Spettl, M. Weber, I. Manke and V. Schmidt, Stochastic 3D modeling of the microstructure of lithium-ion battery anodes via Gaussian random fields on the sphere. *Computational Materials Science* 109 (2015), 137-146.

Anodes of energy cells

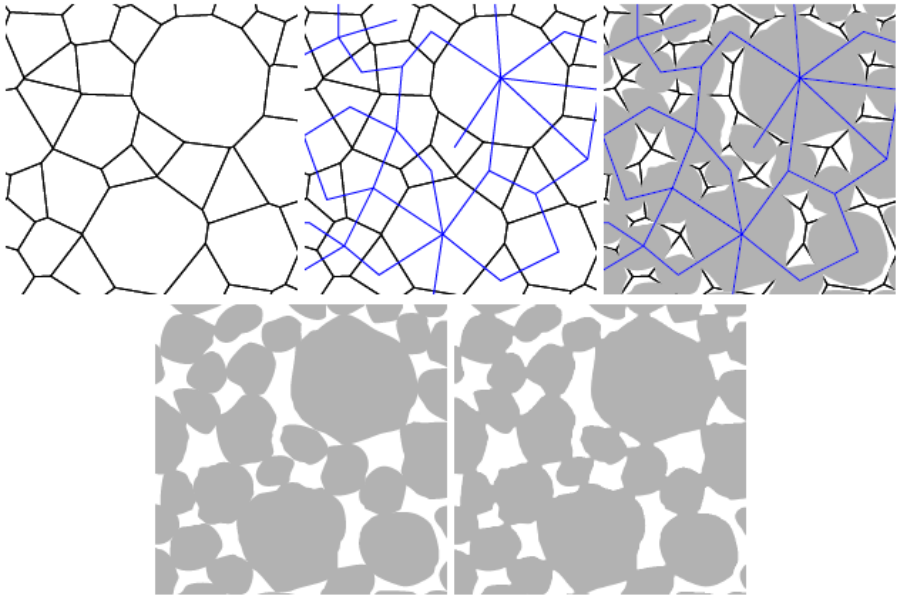

Modeling idea

- decompose ROI in convex polytopes
  $\rightarrow$ Laguerre tessellation
  - resembles sizes and shapes of particles

J. Feinauer, T. Brereton, A. Spettl, M. Weber, I. Manke and V. Schmidt, Stochastic 3D modeling of the microstructure of lithium-ion battery anodes via Gaussian random fields on the sphere. *Computational Materials Science* 109 (2015), 137-146.

Anodes of energy cells

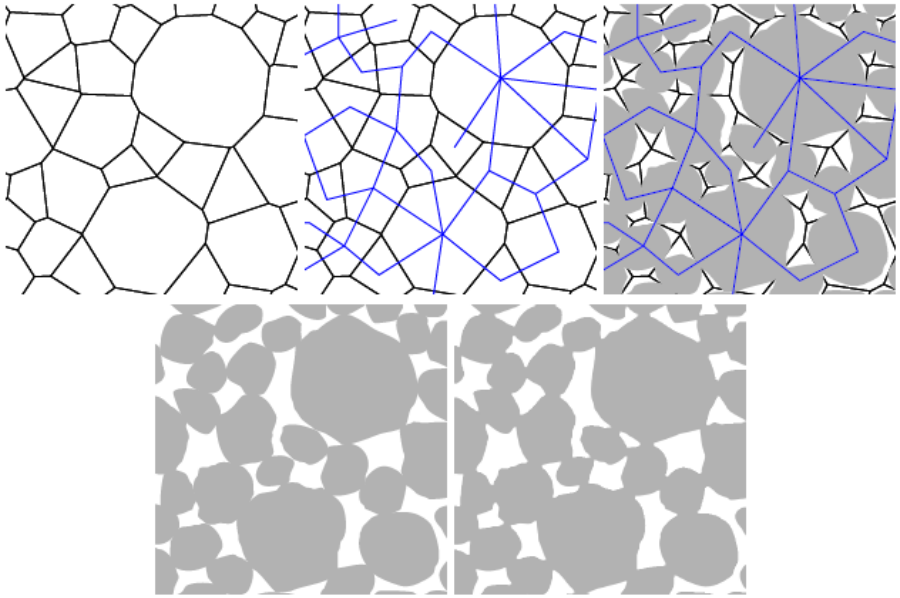

Modeling idea

- decompose ROI in convex polytopes $\rightarrow$ Laguerre tessellation
  - resembles sizes and shapes of particles
- indicate which particles will be connected $\rightarrow$ connectivity graph

J. Feinauer, T. Brereton, A. Spettl, M. Weber, I. Manke and V. Schmidt, Stochastic 3D modeling of the microstructure of lithium-ion battery anodes via Gaussian random fields on the sphere. *Computational Materials Science* 109 (2015), 137-146.

Anodes of energy cells

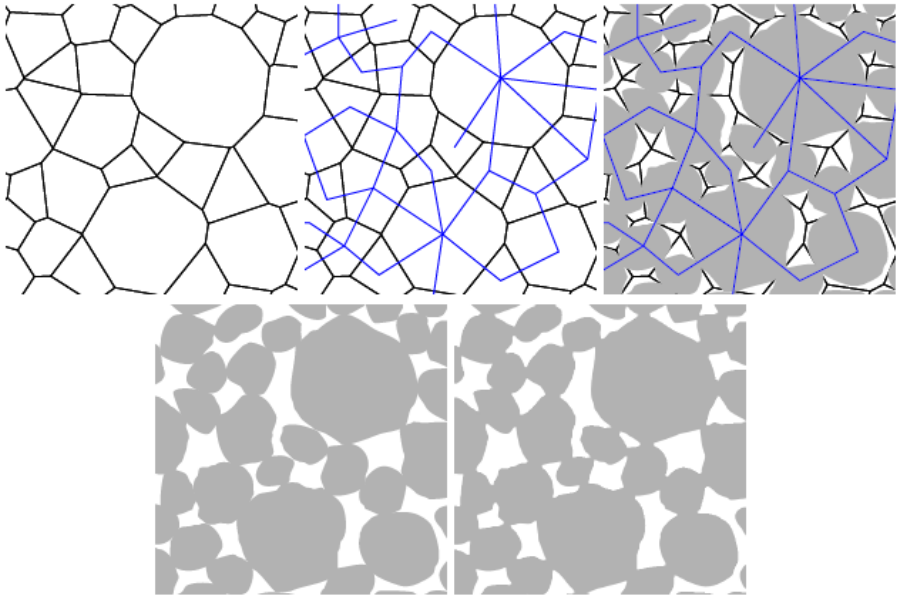

Modeling idea

- decompose ROI in convex polytopes $\rightarrow$ Laguerre tessellation
  - resembles sizes and shapes of particles
- indicate which particles will be connected $\rightarrow$ connectivity graph
- place particles in polytopes $\rightarrow$ random spherical harmonics

J. Feinauer, T. Brereton, A. Spettl, M. Weber, I. Manke and V. Schmidt, Stochastic 3D modeling of the microstructure of lithium-ion battery anodes via Gaussian random fields on the sphere. *Computational Materials Science* 109 (2015), 137-146.

Anodes of energy cells

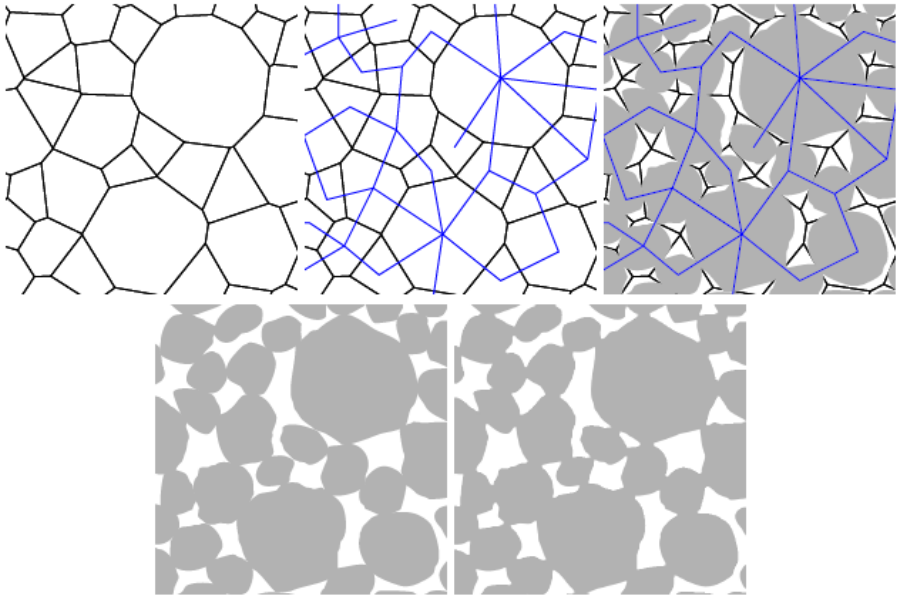

Modeling idea

- decompose ROI in convex polytopes → Laguerre tessellation
  - resembles sizes and shapes of particles
- indicate which particles will be connected → connectivity graph
- place particles in polytopes → random spherical harmonics
- delete tessellation and graph

J. Feinauer, T. Brereton, A. Spettl, M. Weber, I. Manke and V. Schmidt, Stochastic 3D modeling of the microstructure of lithium-ion battery anodes via Gaussian random fields on the sphere. *Computational Materials Science* 109 (2015), 137-146.

Anodes of energy cells

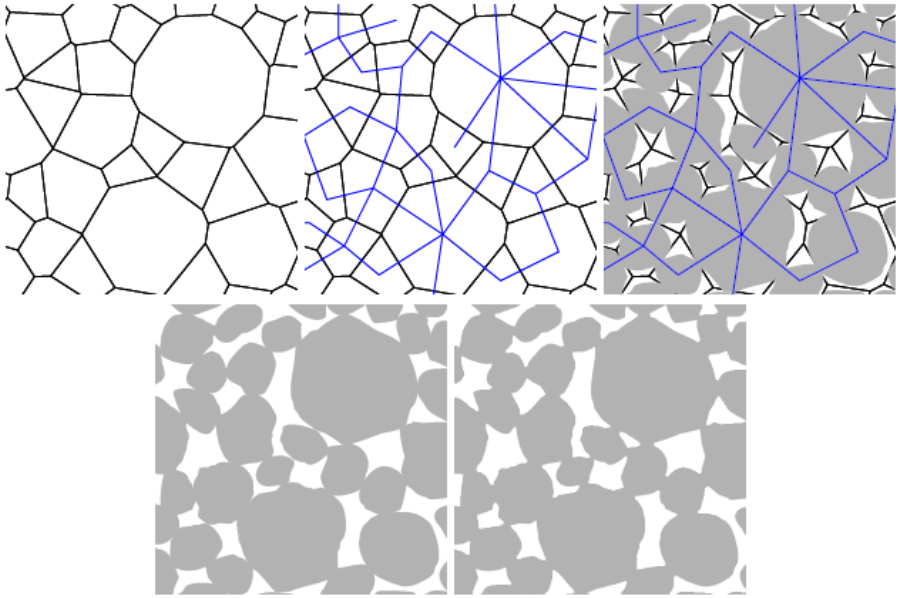

Modeling idea

- decompose ROI in convex polytopes → Laguerre tessellation
  - resembles sizes and shapes of particles
- indicate which particles will be connected → connectivity graph
- place particles in polytopes → random spherical harmonics
- delete tessellation and graph
- mimic effect of binder → morphological smoothing (closing)

J. Feinauer, T. Brereton, A. Spettl, M. Weber, I. Manke and V. Schmidt, Stochastic 3D modeling of the microstructure of lithium-ion battery anodes via Gaussian random fields on the sphere. *Computational Materials Science* 109 (2015), 137-146.

Anodes of energy cells

Validation

Anodes of energy cells

Validation

- spherical contact distance distribution

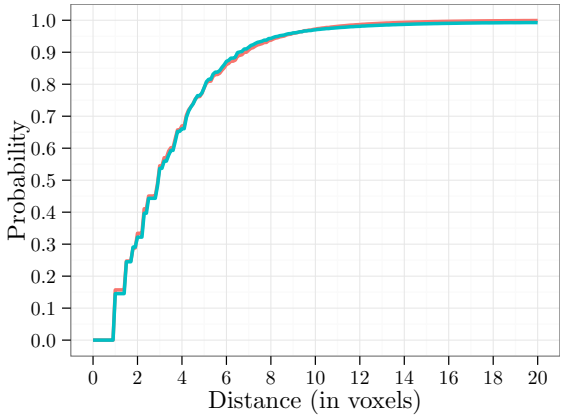

Anodes of energy cells

Validation

- spherical contact distance distribution
- geodesic tortuosity

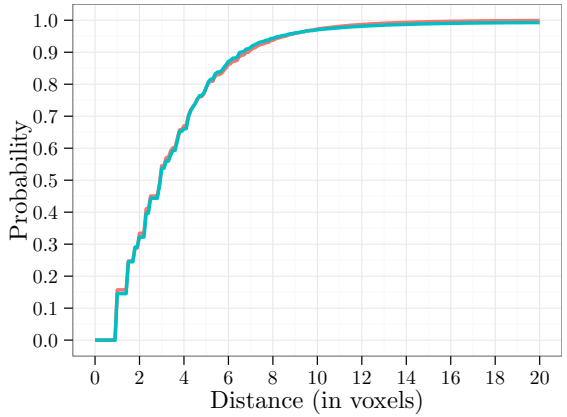

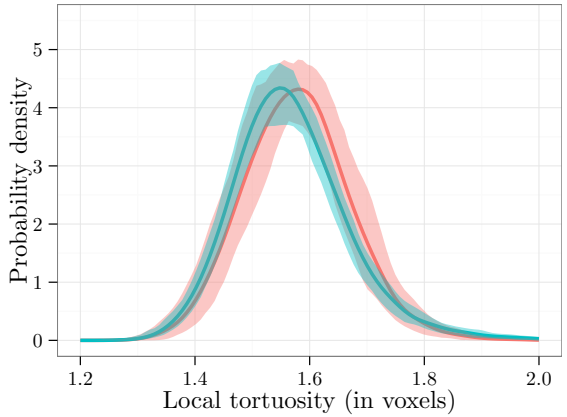

Anodes of energy cells

Validation

- spherical contact distance distribution
- geodesic tortuosity
- ...

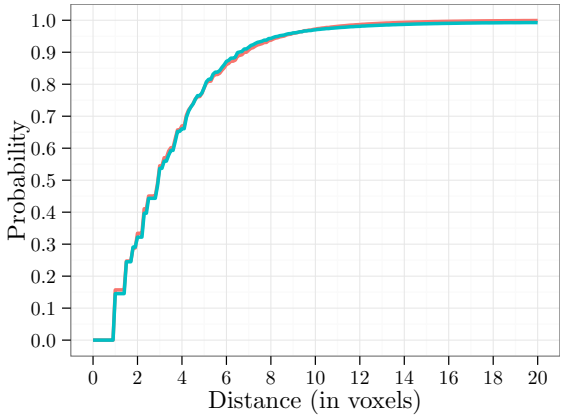

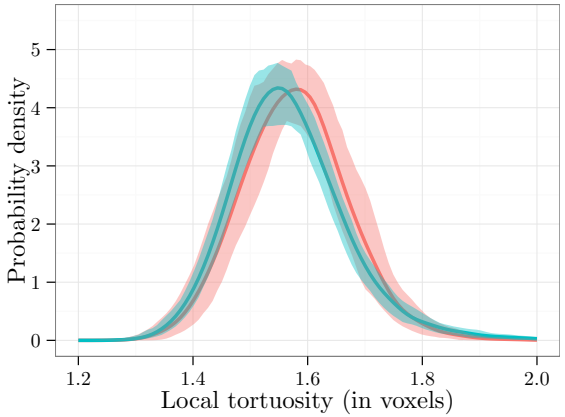

Anodes of energy cells

Electrochemical validation

Anodes of energy cells

Electrochemical validation

- use original and simulated data as input for spatially resolved transport models

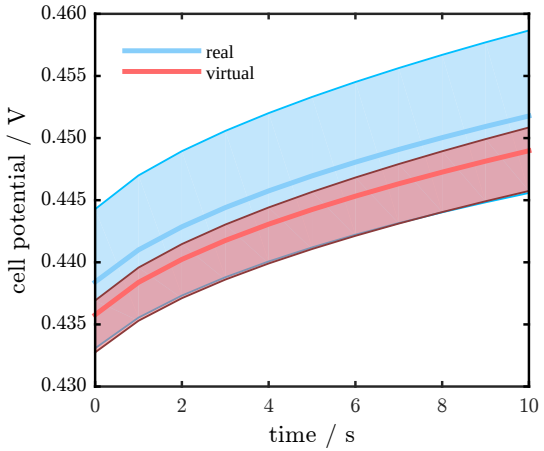

Anodes of energy cells

Electrochemical validation

- use original and simulated data as input for spatially resolved transport models

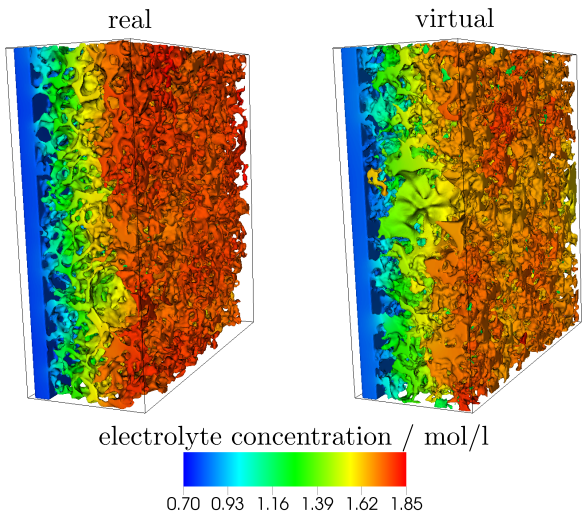

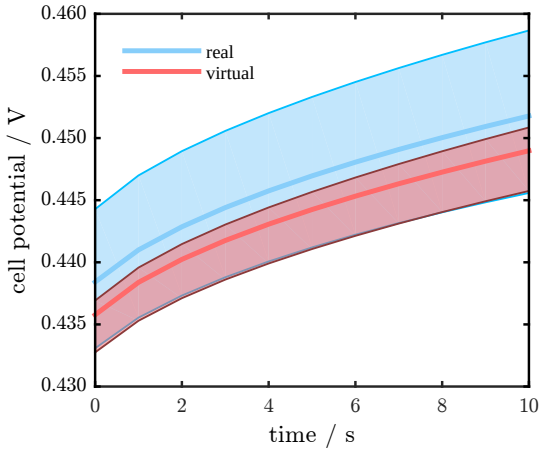

S. Hein, J. Feinauer, D. Westhoff, I. Manke, V. Schmidt and A. Latz, Stochastic microstructure modelling and electrochemical simulation of lithium-ion cell anodes in 3D. *Journal of Power Sources* (submitted).

Anodes of energy cells

Electrochemical validation

- use original and simulated data as input for spatially resolved transport models
  - electrolyte concentration

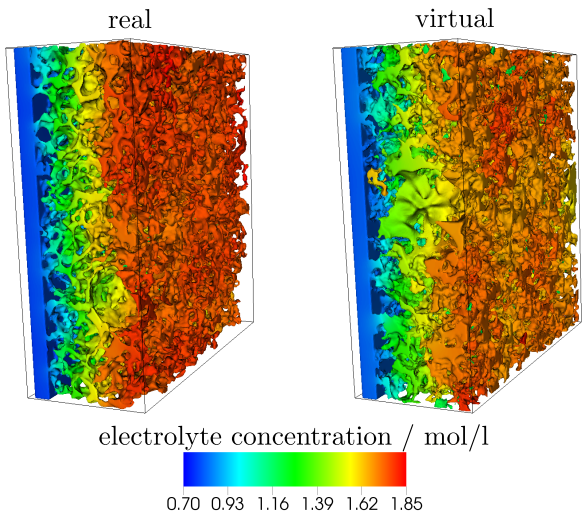

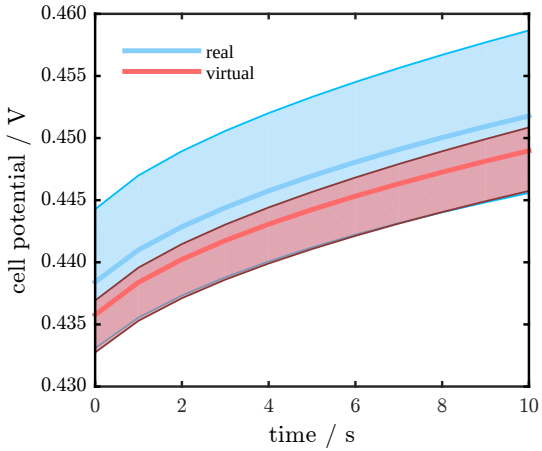

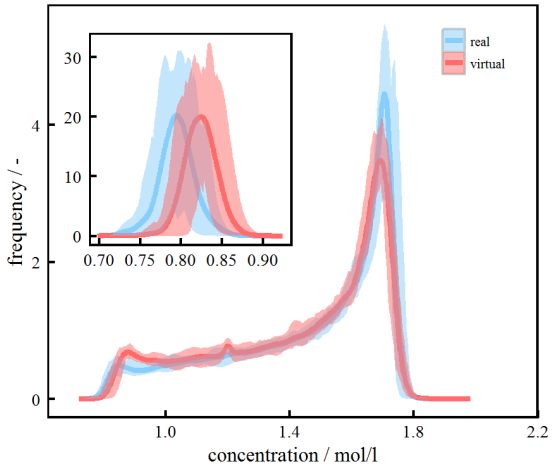

S. Hein, J. Feinauer, D. Westhoff, I. Manke, V. Schmidt and A. Latz, Stochastic microstructure modelling and electrochemical simulation of lithium-ion cell anodes in 3D. *Journal of Power Sources* (submitted).

Anodes of energy cells

Electrochemical validation

- use original and simulated data as input for spatially resolved transport models
  - electrolyte concentration
  - current density

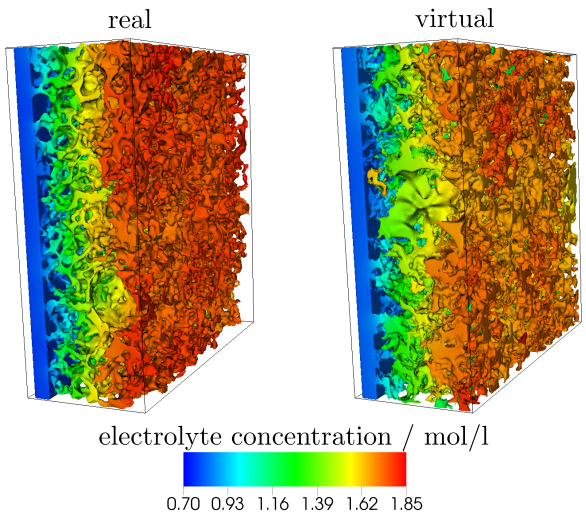

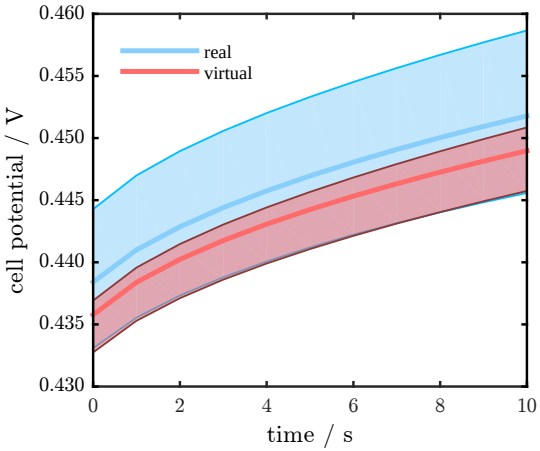

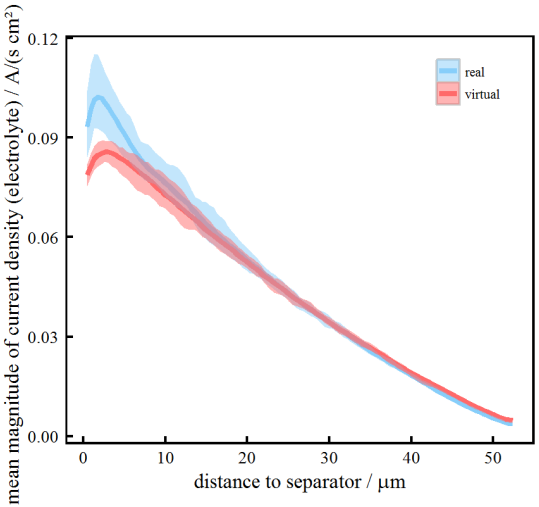

S. Hein, J. Feinauer, D. Westhoff, I. Manke, V. Schmidt and A. Latz, Stochastic microstructure modelling and electrochemical simulation of lithium-ion cell anodes in 3D. *Journal of Power Sources* (submitted).

Anodes of energy cells

Electrochemical validation

- use original and simulated data as input for spatially resolved transport models
  - electrolyte concentration
  - current density
  - overpotential

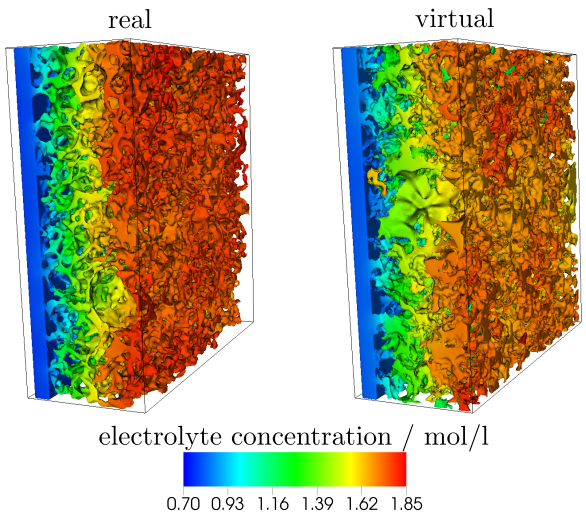

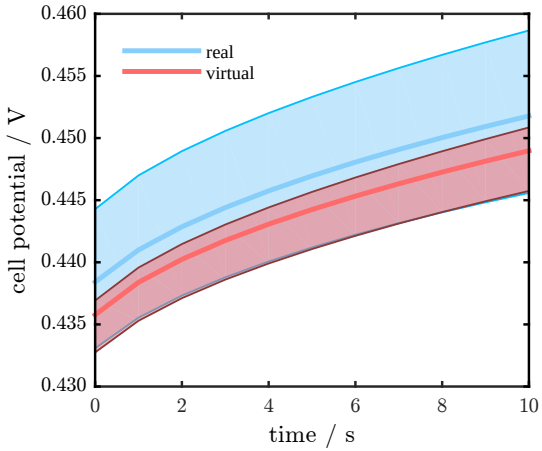

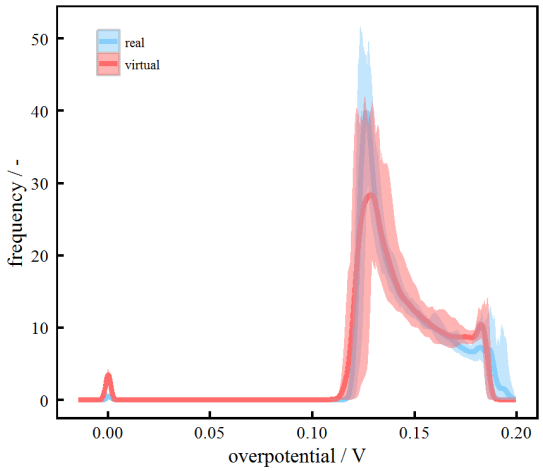

S. Hein, J. Feinauer, D. Westhoff, I. Manke, V. Schmidt and A. Latz, Stochastic microstructure modelling and electrochemical simulation of lithium-ion cell anodes in 3D. *Journal of Power Sources* (submitted).

Anodes of energy cells

Electrochemical validation

- use original and simulated data as input for spatially resolved transport models
  - electrolyte concentration
  - current density
  - overpotential
  - ...

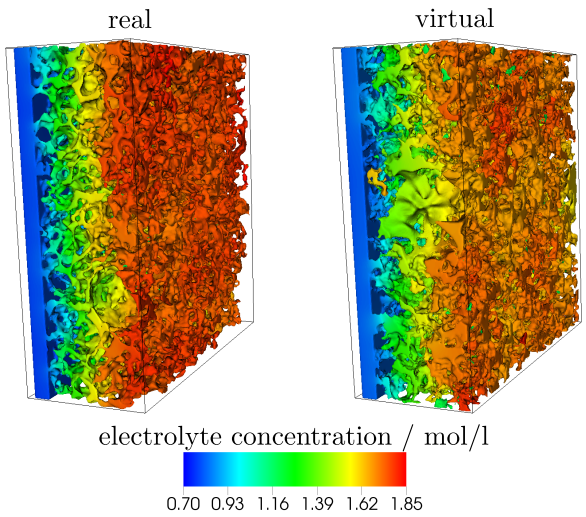

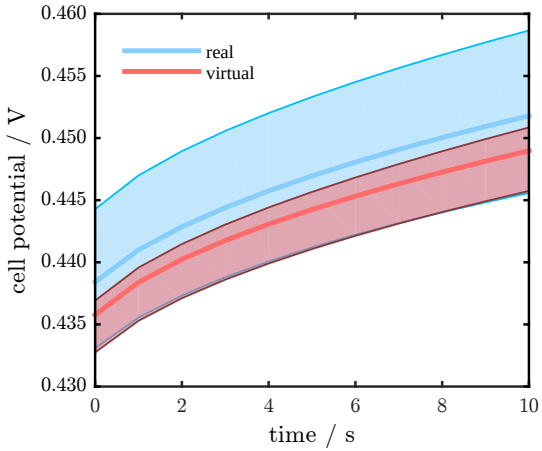

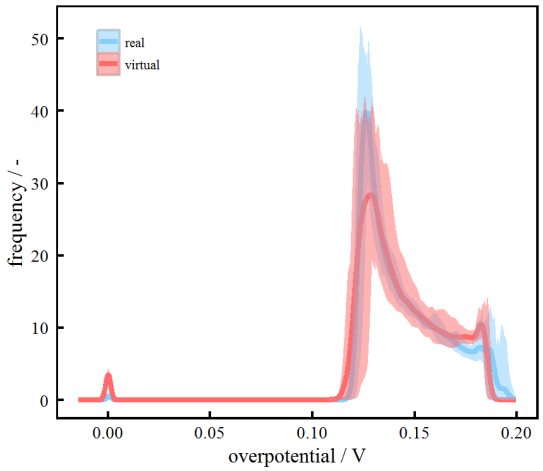

S. Hein, J. Feinauer, D. Westhoff, I. Manke, V. Schmidt and A. Latz, Stochastic microstructure modelling and electrochemical simulation of lithium-ion cell anodes in 3D. *Journal of Power Sources* (submitted).

Anodes of power cells

Anodes of power cells

Main structural differences

Anodes of power cells

Main structural differences

- much lower volume fraction of solid phase

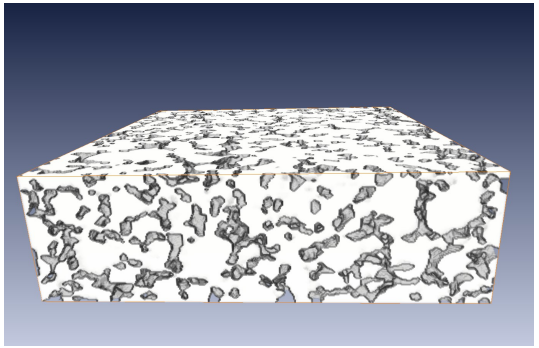

Energy cell anode

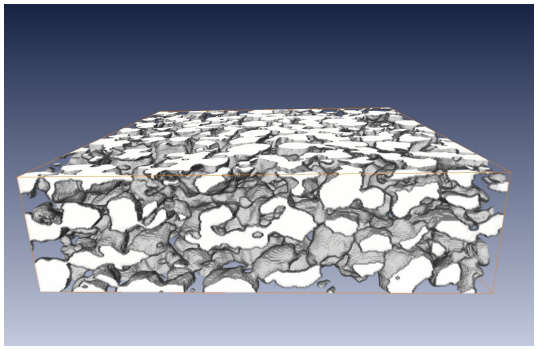

Power cell anode

Anodes of power cells

Main structural differences

- much lower volume fraction of solid phase
- anisotropic morphology

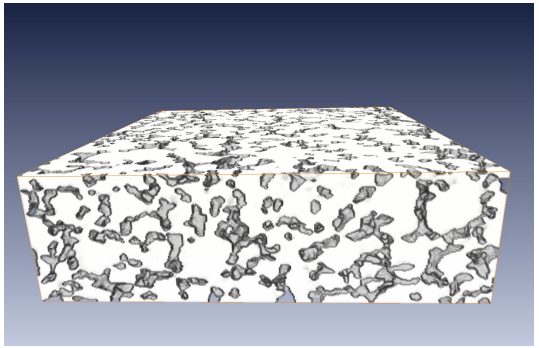

Energy cell anode

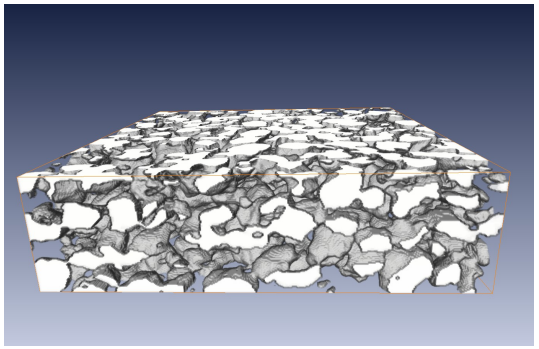

Power cell anode

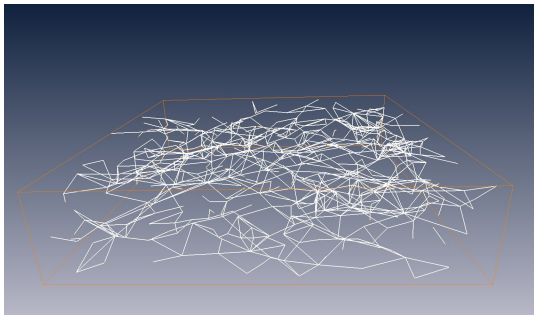

Extracted connectivity graph

Anodes of power cells

Main structural differences

- much lower volume fraction of solid phase
- anisotropic morphology
- more irregularly shaped particles

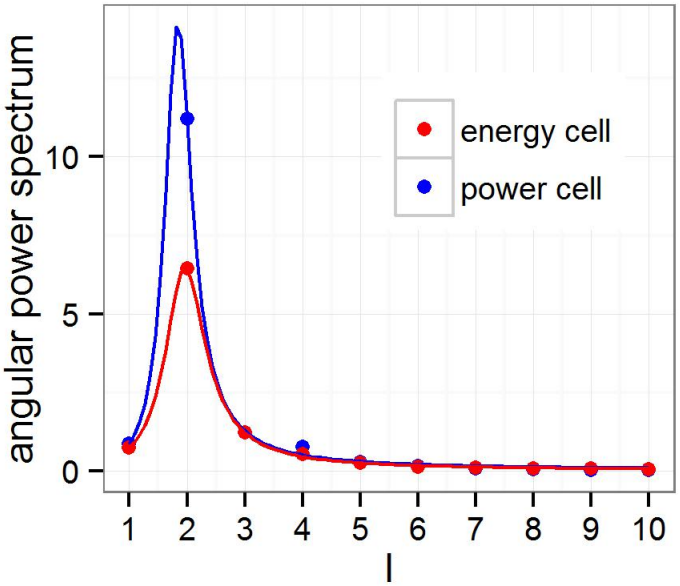

Increased variances of normally distributed coefficiencts c_l^m

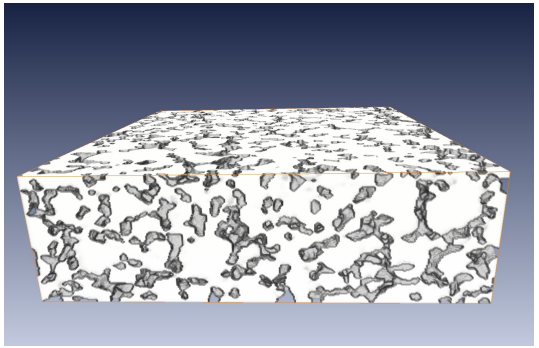

Energy cell anode

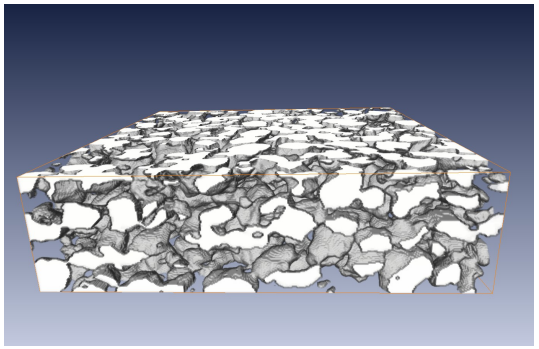

Power cell anode

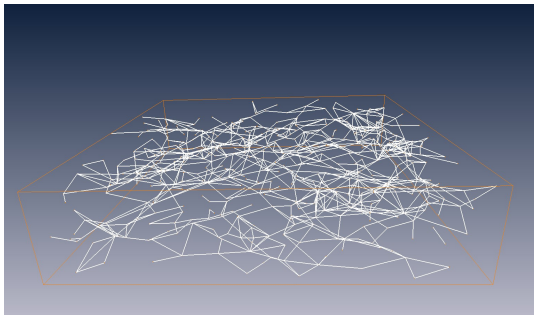

Extracted connectivity graph

Anodes of power cells

D. Westhoff, J. Feinauer, K. Kuchler, T. Mitsch, I. Manke and V. Schmidt, Parametric stochastic 3D model for the microstructure of anodes in lithium-ion power cells. *Computational Materials Science* (under revision)

Anodes of power cells

Match lower volume fraction

D. Westhoff, J. Feinauer, K. Kuchler, T. Mitsch, I. Manke and V. Schmidt, Parametric stochastic 3D model for the microstructure of anodes in lithium-ion power cells. *Computational Materials Science* (under revision)

Anodes of power cells

Match lower volume fraction

- direct use of energy cell model impossible → decreased volume fraction would lead to atypcial particle shapes

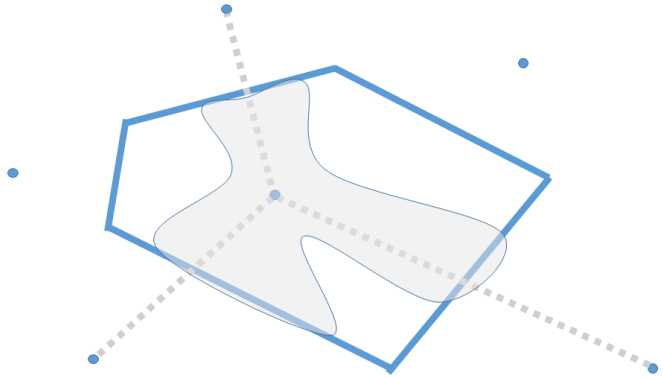

D. Westhoff, J. Feinauer, K. Kuchler, T. Mitsch, I. Manke and V. Schmidt, Parametric stochastic 3D model for the microstructure of anodes in lithium-ion power cells. *Computational Materials Science* (under revision)

Anodes of power cells

Match lower volume fraction

- direct use of energy cell model impossible → decreased volume fraction would lead to atypcial particle shapes
- solution: allow empty polytopes

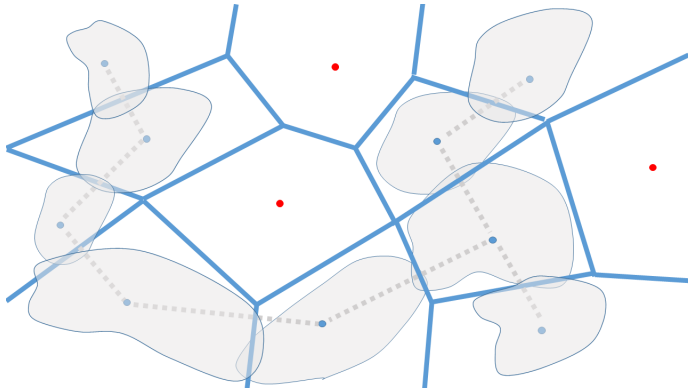

D. Westhoff, J. Feinauer, K. Kuchler, T. Mitsch, I. Manke and V. Schmidt, Parametric stochastic 3D model for the microstructure of anodes in lithium-ion power cells. *Computational Materials Science* (under revision)

Anodes of power cells

Match lower volume fraction

- direct use of energy cell model impossible → decreased volume fraction would lead to atypcial particle shapes
- solution: allow empty polytopes

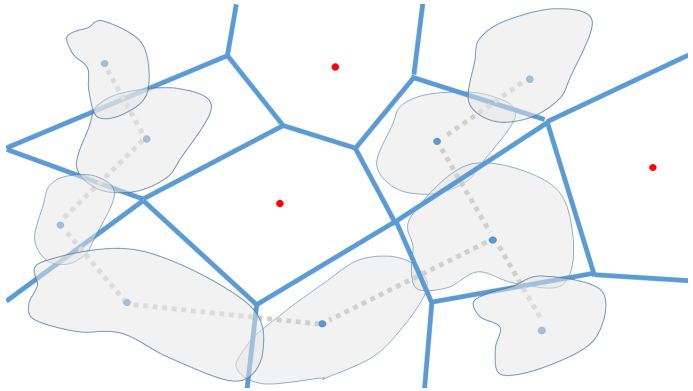

Include anisotropy effects

D. Westhoff, J. Feinauer, K. Kuchler, T. Mitsch, I. Manke and V. Schmidt, Parametric stochastic 3D model for the microstructure of anodes in lithium-ion power cells. *Computational Materials Science* (under revision)

Anodes of power cells

Match lower volume fraction

- direct use of energy cell model impossible → decreased volume fraction would lead to atypcial particle shapes
- solution: allow empty polytopes

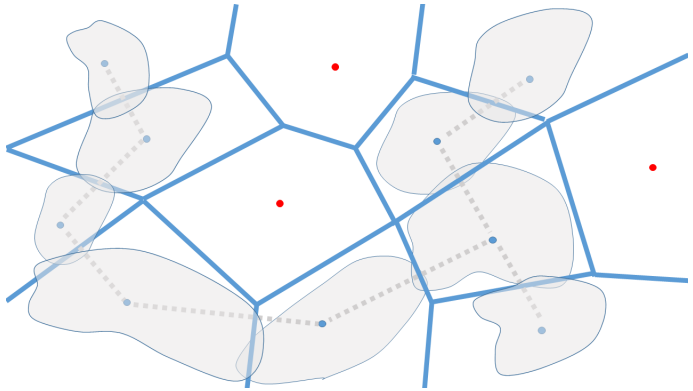

Include anisotropy effects

- solid phase is compressed vertically

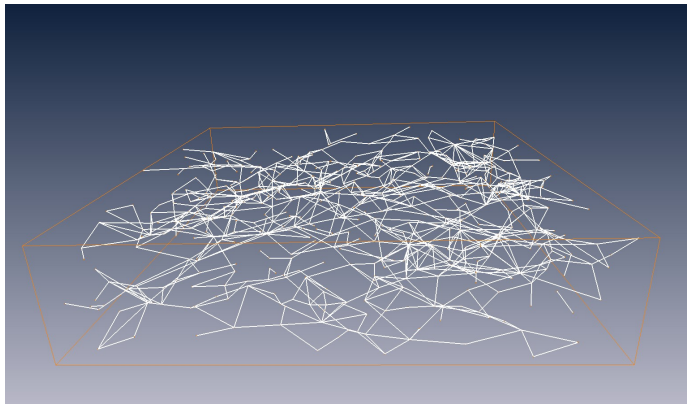

D. Westhoff, J. Feinauer, K. Kuchler, T. Mitsch, I. Manke and V. Schmidt, Parametric stochastic 3D model for the microstructure of anodes in lithium-ion power cells. *Computational Materials Science* (under revision)

Anodes of power cells

Match lower volume fraction

- direct use of energy cell model impossible → decreased volume fraction would lead to atypcial particle shapes
- solution: allow empty polytopes

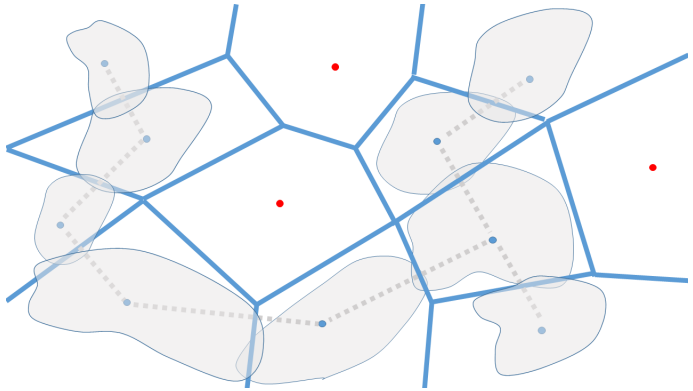

Include anisotropy effects

- solid phase is compressed vertically
- solution: anisotropic connectivity graph

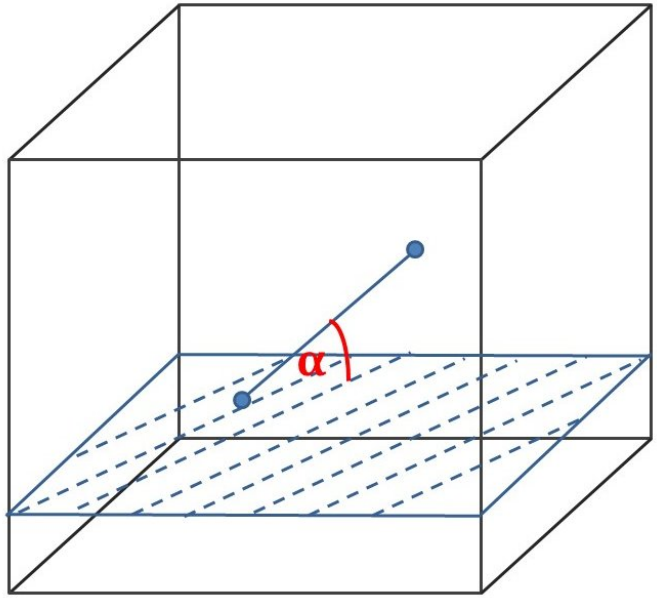

D. Westhoff, J. Feinauer, K. Kuchler, T. Mitsch, I. Manke and V. Schmidt, Parametric stochastic 3D model for the microstructure of anodes in lithium-ion power cells. *Computational Materials Science* (under revision)

Anodes of power cells

Match lower volume fraction

- direct use of energy cell model impossible → decreased volume fraction would lead to atypcial particle shapes
- solution: allow empty polytopes

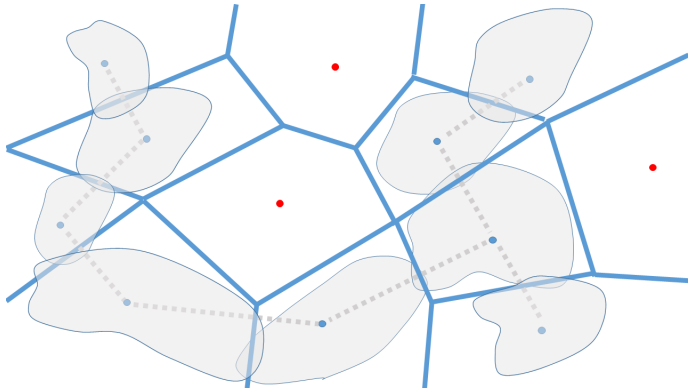

Include anisotropy effects

- solid phase is compressed vertically
- solution: anisotropic connectivity graph

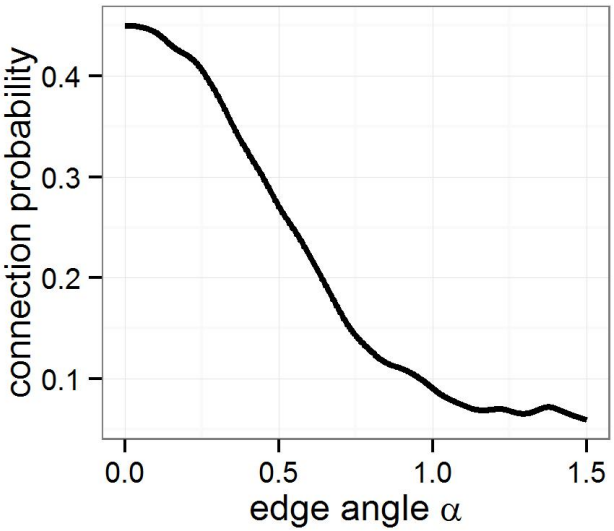

D. Westhoff, J. Feinauer, K. Kuchler, T. Mitsch, I. Manke and V. Schmidt, Parametric stochastic 3D model for the microstructure of anodes in lithium-ion power cells. *Computational Materials Science* (under revision)

Anodes of power cells

Match lower volume fraction

- direct use of energy cell model impossible → decreased volume fraction would lead to atypcial particle shapes
- solution: allow empty polytopes

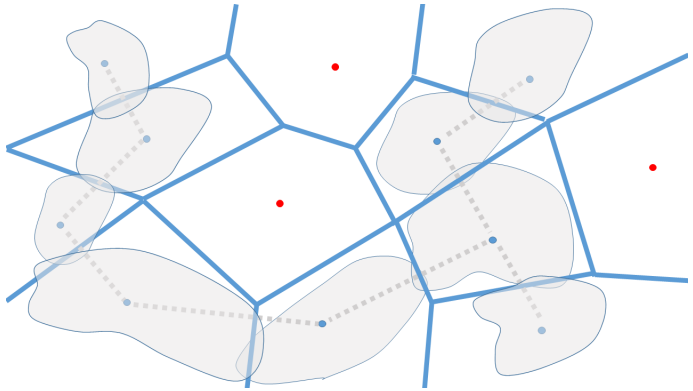

Include anisotropy effects

- solid phase is compressed vertically
- solution: anisotropic connectivity graph

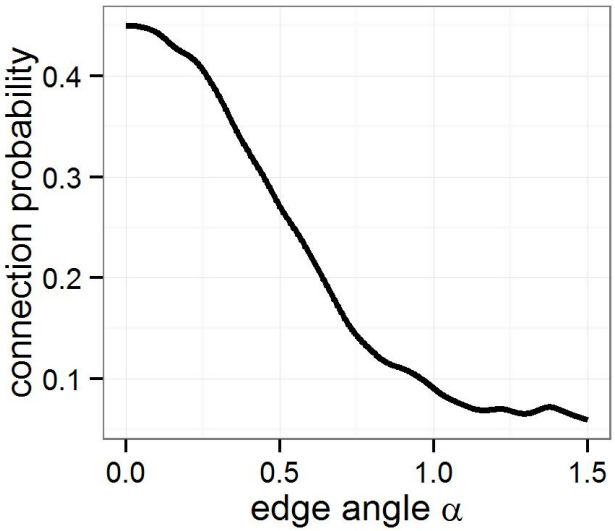

Handle more irregular particle shapes

- solution: more flexible boundary conditions in combination with smaller L

D. Westhoff, J. Feinauer, K. Kuchler, T. Mitsch, I. Manke and V. Schmidt, Parametric stochastic 3D model for the microstructure of anodes in lithium-ion power cells. *Computational Materials Science* (under revision)

Anodes of power cells

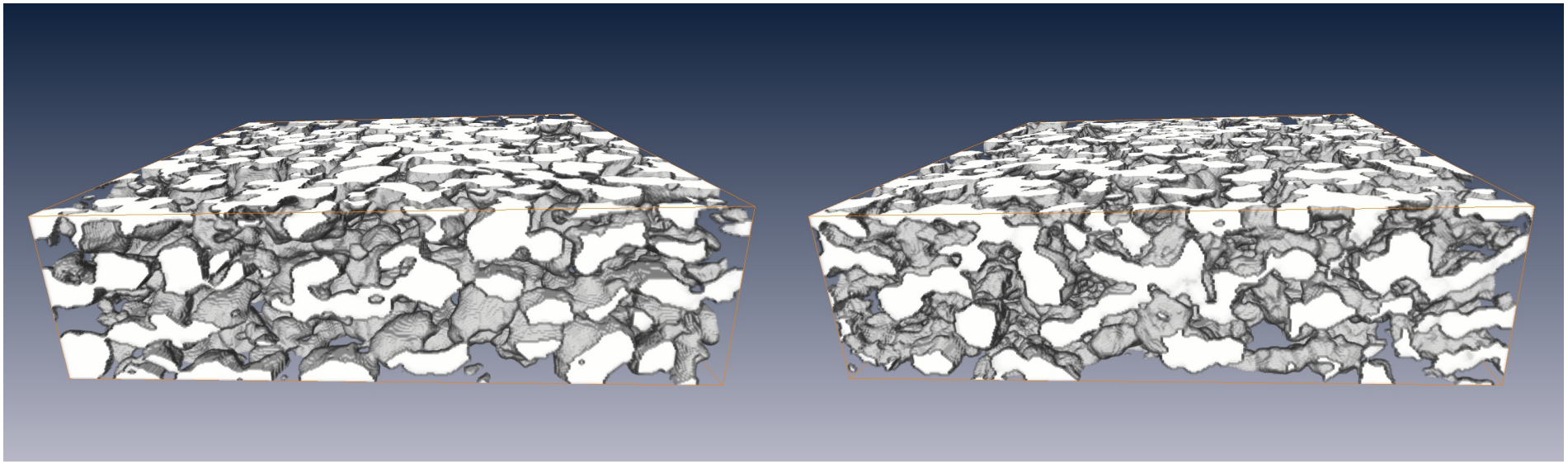

experimental data simulated data

Anodes of power cells

Anodes of power cells

Validation

Anodes of power cells

Validation

- volume fraction

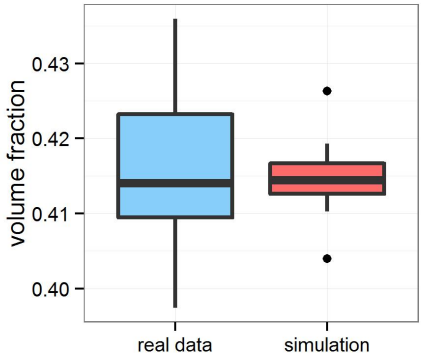

Anodes of power cells

Validation

- volume fraction
- specific surface area

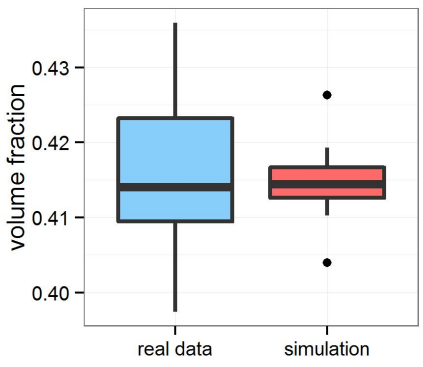

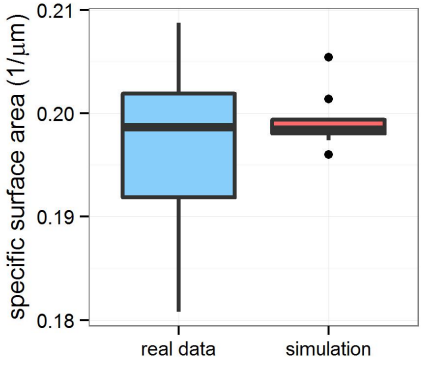

Anodes of power cells

Validation

- volume fraction
- specific surface area
- geodesic tortuosity

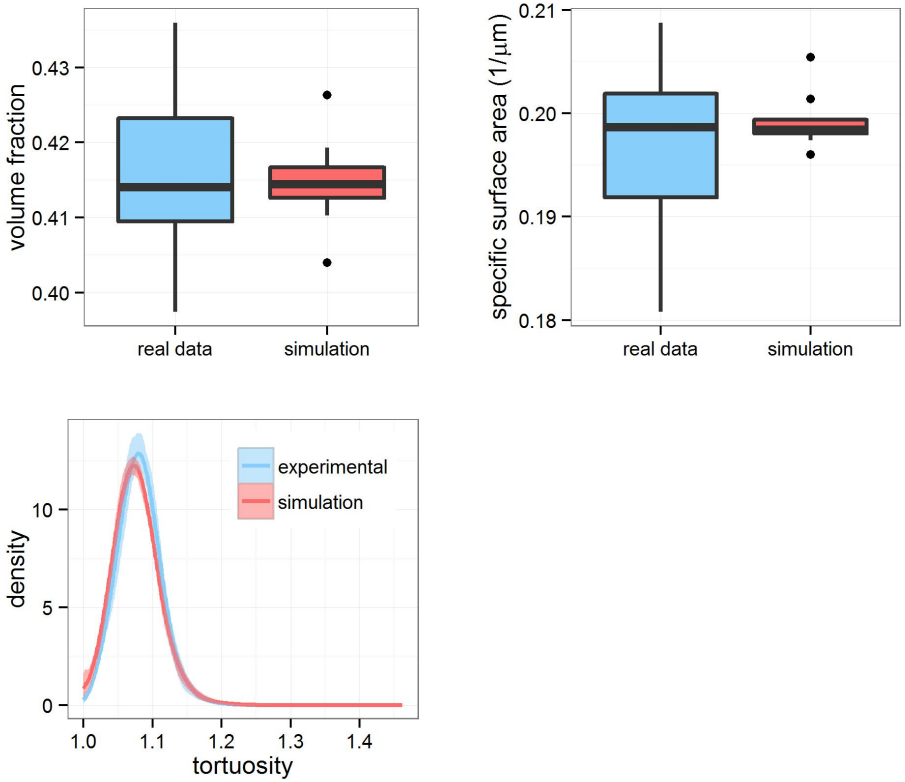

Anodes of power cells

Validation

- volume fraction
- specific surface area
- geodesic tortuosity
- cell potential

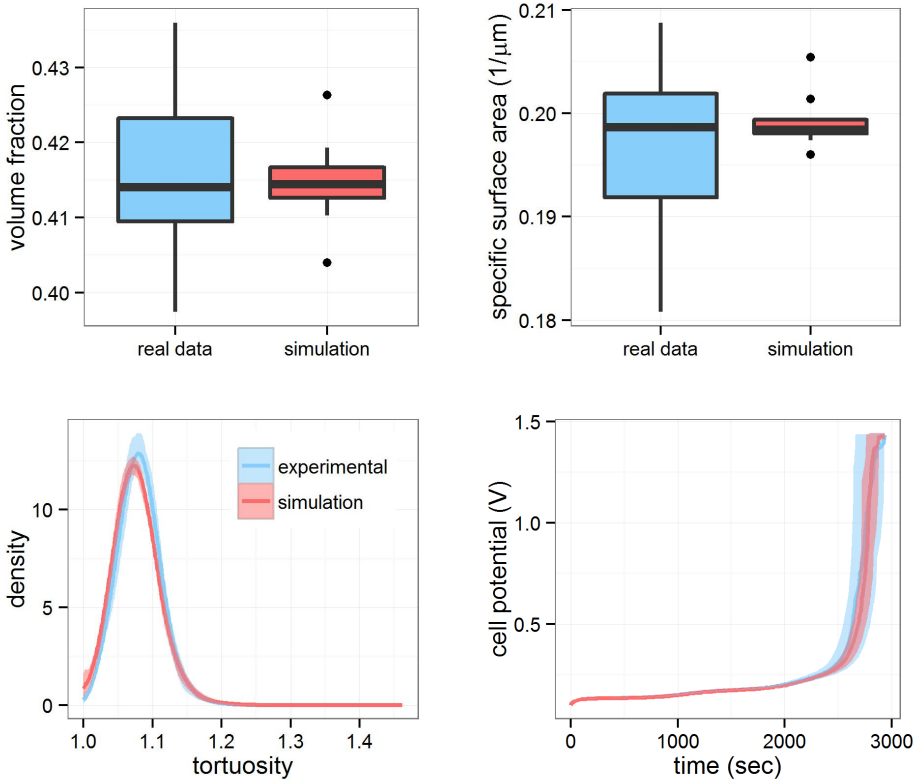

Application of the model

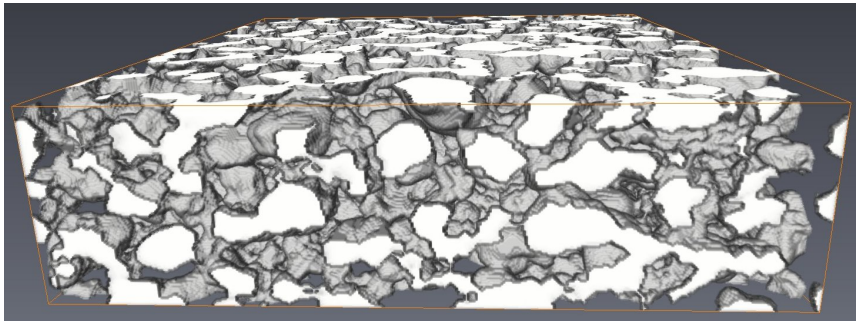

Application of the model

Create virtual structures

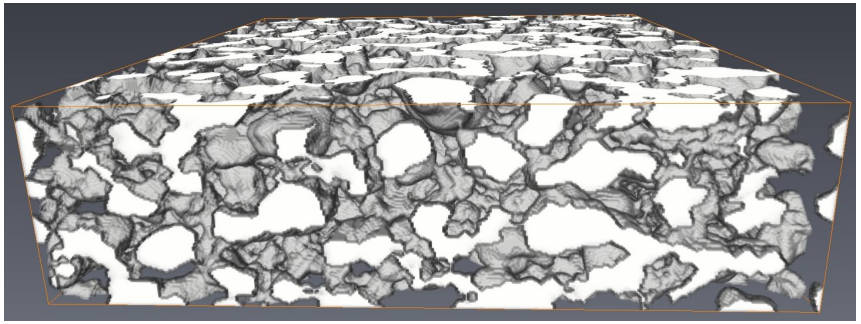

Application of the model

Create virtual structures

- higher volume fraction of solid phase

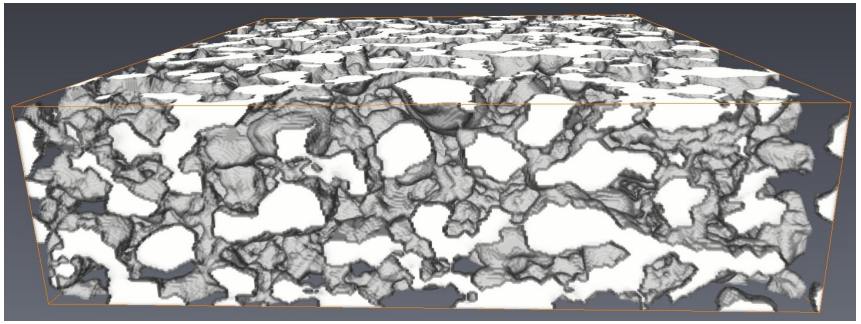

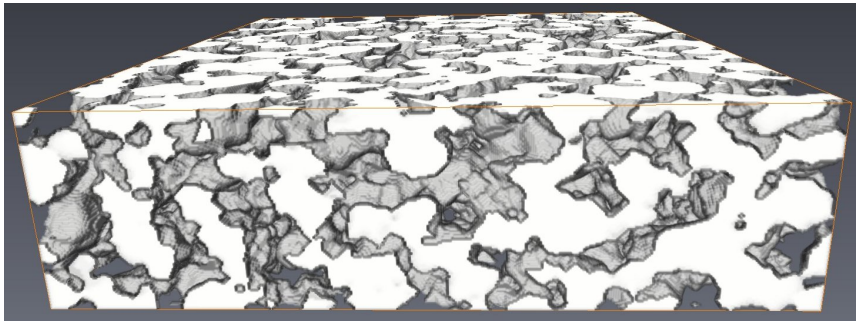

Application of the model

Create virtual structures

- higher volume fraction of solid phase
- more pronounced anisotropy effects

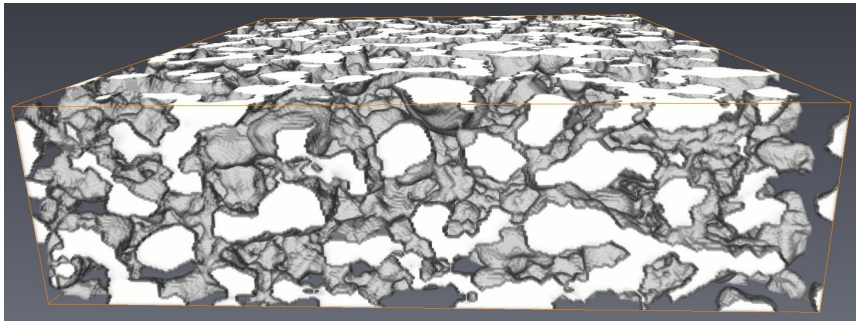

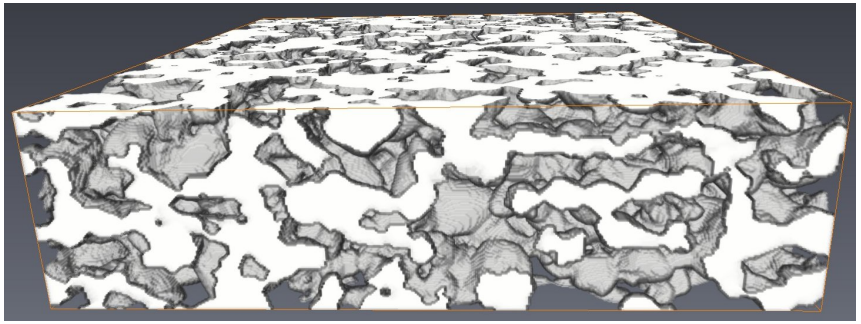

Application of the model

Create virtual structures

- higher volume fraction of solid phase
- more pronounced anisotropy effects
- no anisotropy effects

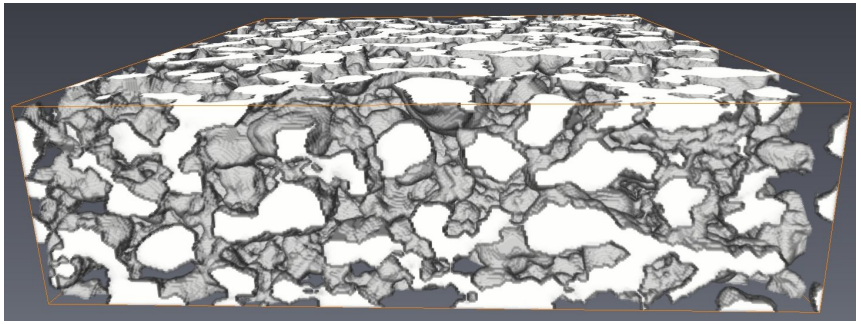

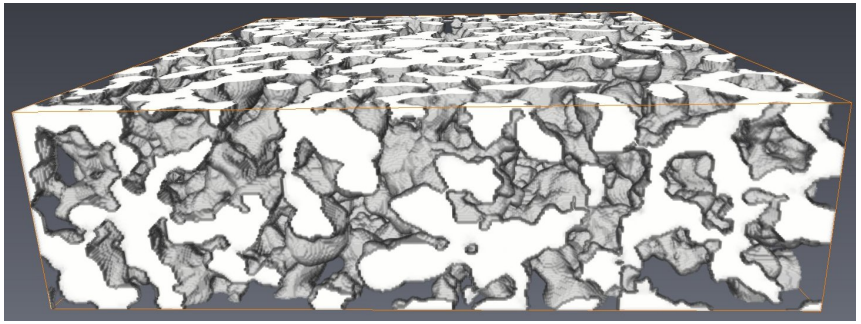

Application of the model

Create virtual structures

- higher volume fraction of solid phase
- more pronounced anisotropy effects
- no anisotropy effects
- structural gradient

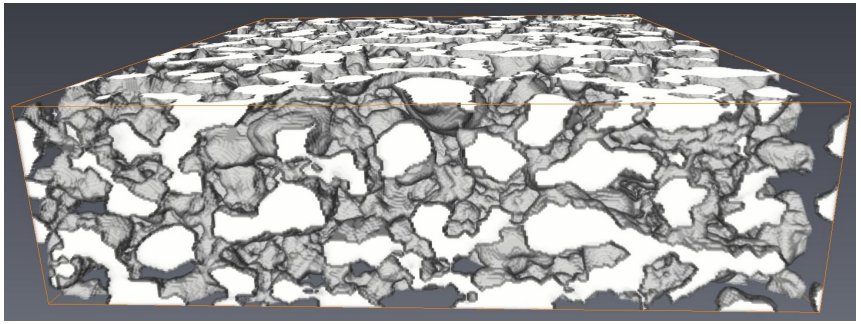

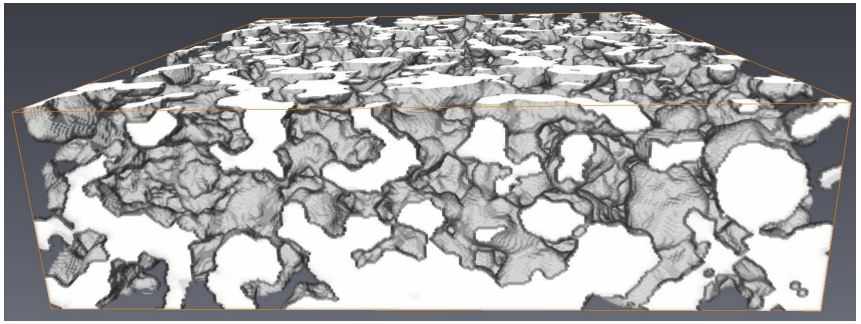

Application of the model

Create virtual structures

- higher volume fraction of solid phase
- more pronounced anisotropy effects
- no anisotropy effects
- structural gradient

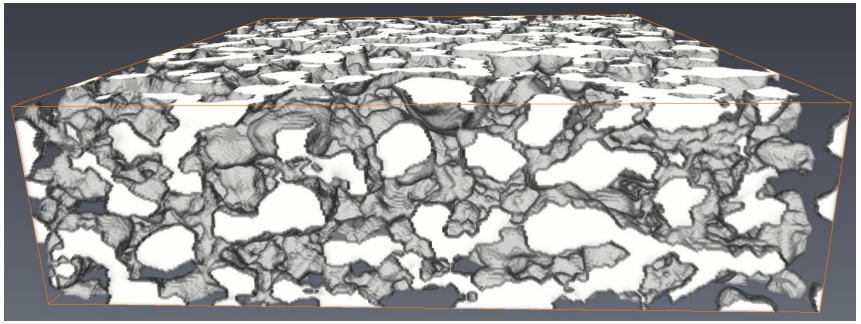

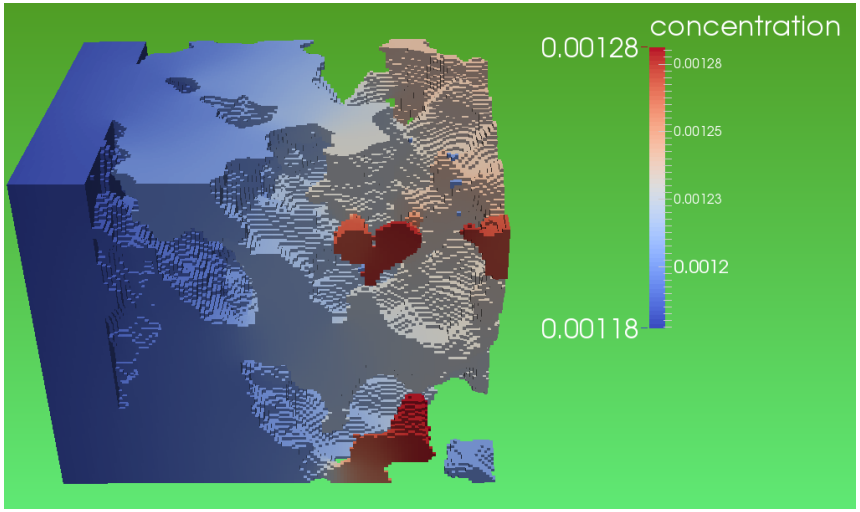

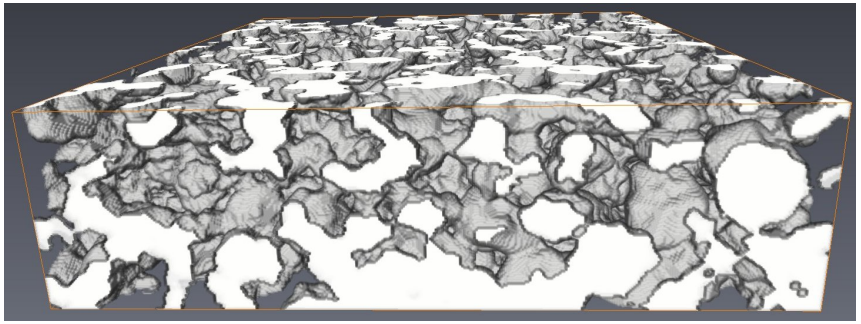

Stochastic modeling of agglomerates

Aim

- realistic model for the random 3D structure of agglomerates
- use model to analyze breakage behavior

Requirements

- spherical primary particles without overlap
- bonds: primary particles are connected by solid bridges
- parameters of the model should be linked to the experiment
  - porosity of agglomerates
  - radii of primary particles
  - volume of binder material

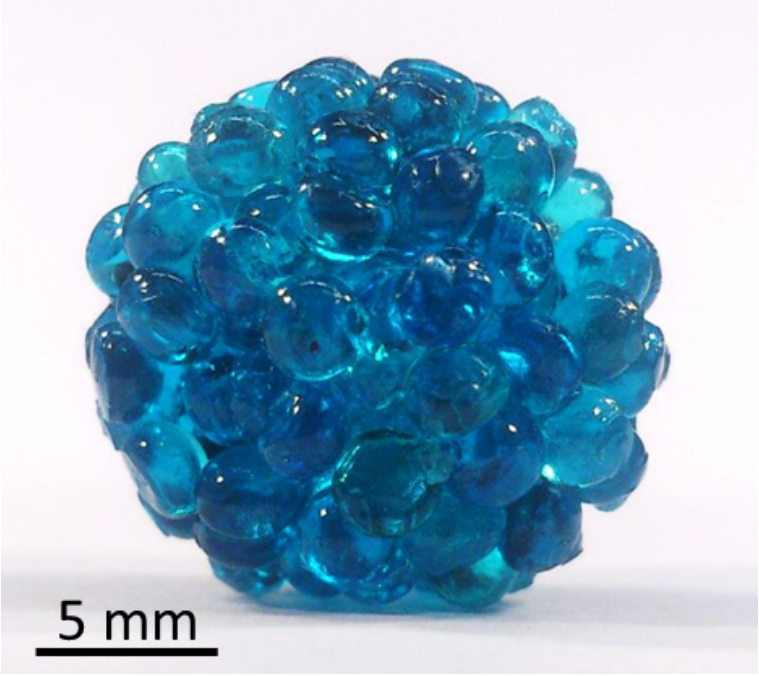

Stochastic modeling of the 3D microstructure

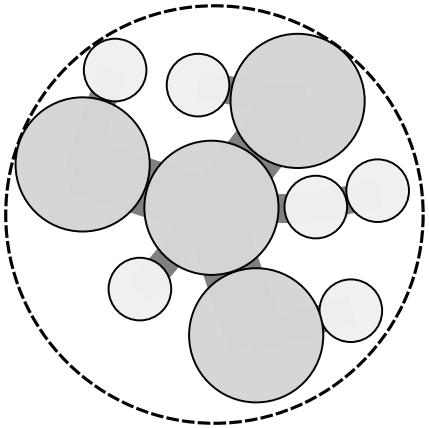

1. random agglomerate shape
2. initial structure of overlapping primary particles
3. collective rearrangement of primary particles
4. bond network

A. Spettl, M. Dosta, S. Antonyuk, S. Heinrich and V. Schmidt, Statistical investigation of agglomerate breakage based on combined stochastic microstructure modeling and DEM simulations. *Advanced Powder Technology* 26 (2015), 1021–1030.

Stochastic modeling of the 3D microstructure

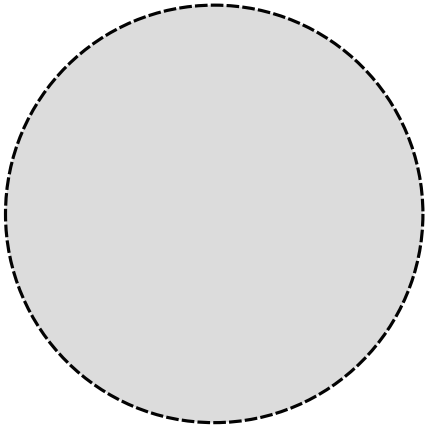

1. random agglomerate shape
   - realization D of $\mathbb{D}$
   - example: $\mathbb{D} = B_3(o, R_D)$ for a random radius R_D
2. initial structure of overlapping primary particles
3. collective rearrangement of primary particles
4. bond network

Stochastic modeling of the 3D microstructure

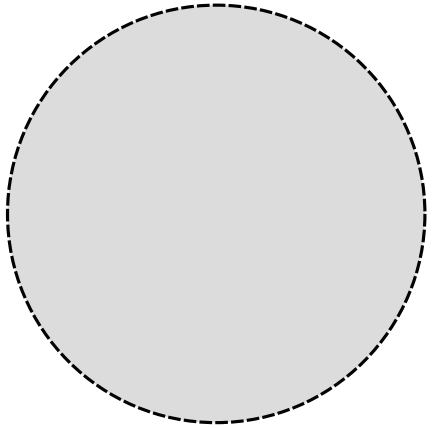

1. random agglomerate shape
2. initial structure of overlapping primary particles
3. collective rearrangement of primary particles
4. bond network

Stochastic modeling of the 3D microstructure

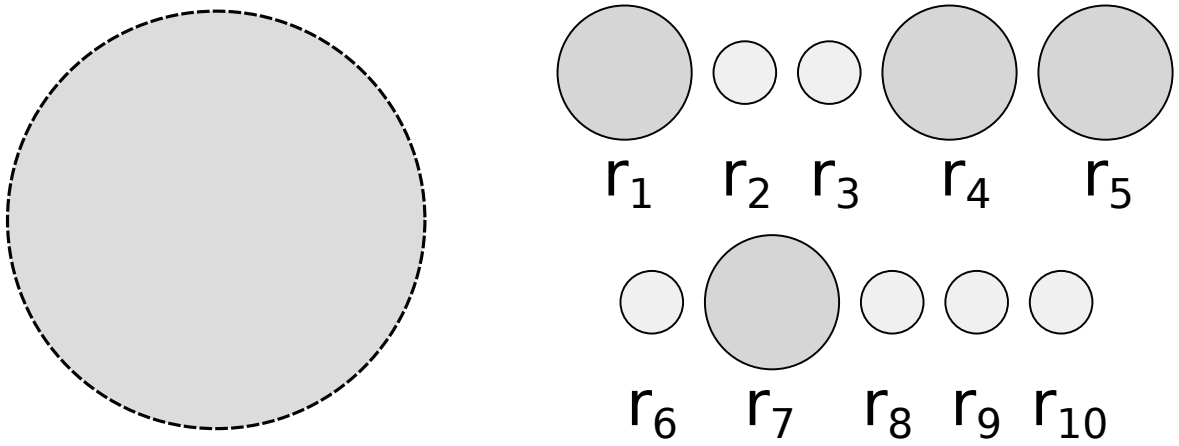

1. random agglomerate shape
2. initial structure of overlapping primary particles
   - radii r_i: realizations of R_i, $i = 1, 2, \ldots$, with R_i independent and F_{R_p}-distributed
   - packing density η: realization of $\mathbb{H}$
   - number of particles $n \in \mathbb{N}$: $\sum_{i=1}^{n} \frac{4}{3}\pi r_i^3 \approx \eta\, \nu_3(D)$
3. collective rearrangement of primary particles
4. bond network

Stochastic modeling of the 3D microstructure

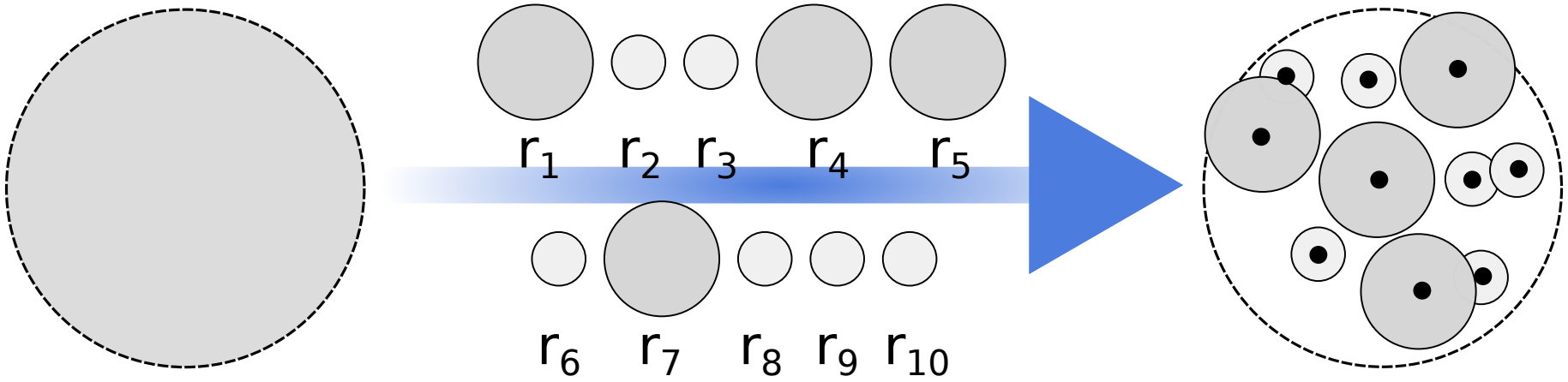

1. random agglomerate shape
2. initial structure of overlapping primary particles
   - radii r_i: realizations of R_i, $i = 1, 2, \ldots$, with R_i independent and F_{R_p}-distributed
   - packing density η: realization of $\mathbb{H}$
   - number of particles $n \in \mathbb{N}$: $\sum_{i=1}^{n} \frac{4}{3}\pi r_i^3 \approx \eta\, \nu_3(D)$
   - centers s_i: realizations of S_i, $i = 1, \ldots, n$, with S_i independent and $U(D)$-distributed
3. collective rearrangement of primary particles
4. bond network

Stochastic modeling of the 3D microstructure

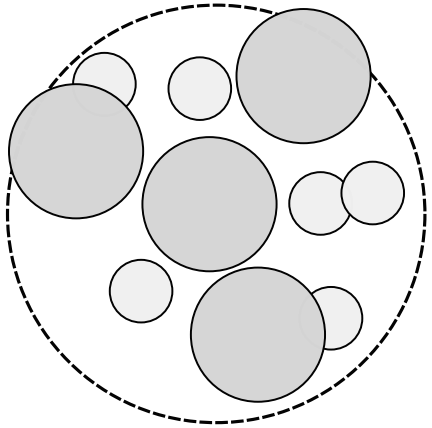

1. random agglomerate shape
2. initial structure of overlapping primary particles
3. collective rearrangement of primary particles
4. bond network

Stochastic modeling of the 3D microstructure

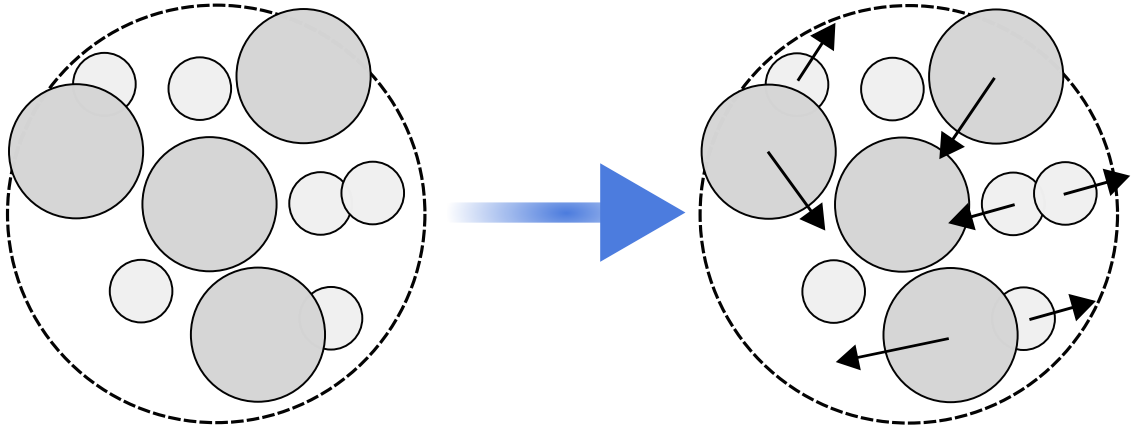

1. random agglomerate shape
2. initial structure of overlapping primary particles
3. collective rearrangement of primary particles
   - deterministic procedure: application of the force-biased algorithm
4. bond network

Stochastic modeling of the 3D microstructure

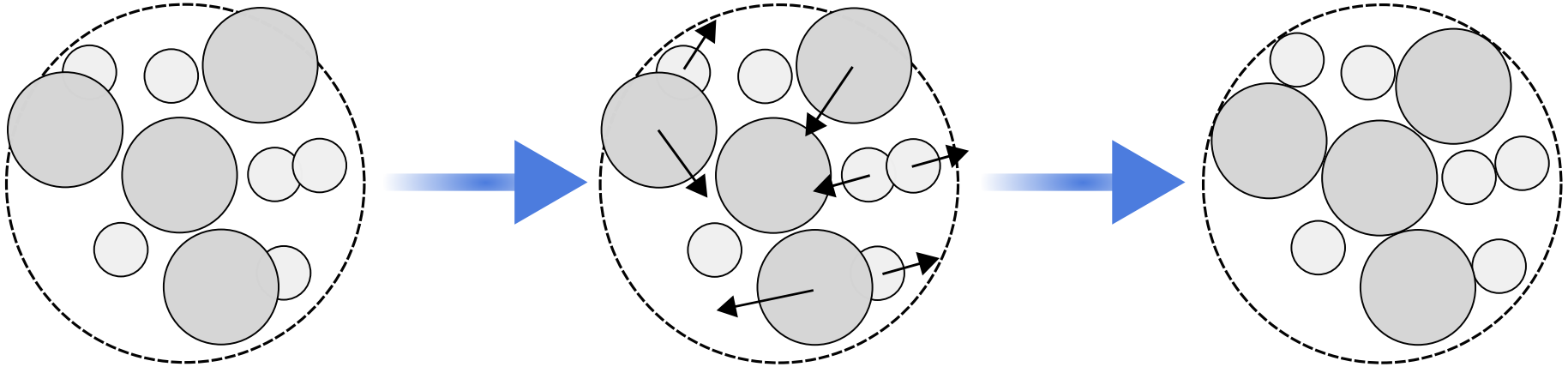

1. random agglomerate shape
2. initial structure of overlapping primary particles
3. collective rearrangement of primary particles
   - deterministic procedure: application of the force-biased algorithm
4. bond network

Stochastic modeling of the 3D microstructure

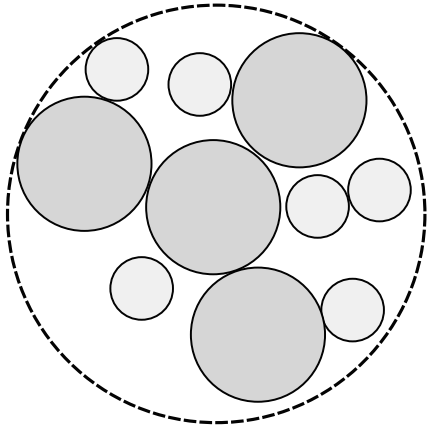

1. random agglomerate shape
2. initial structure of overlapping primary particles
3. collective rearrangement of primary particles
4. bond network

Stochastic modeling of the 3D microstructure

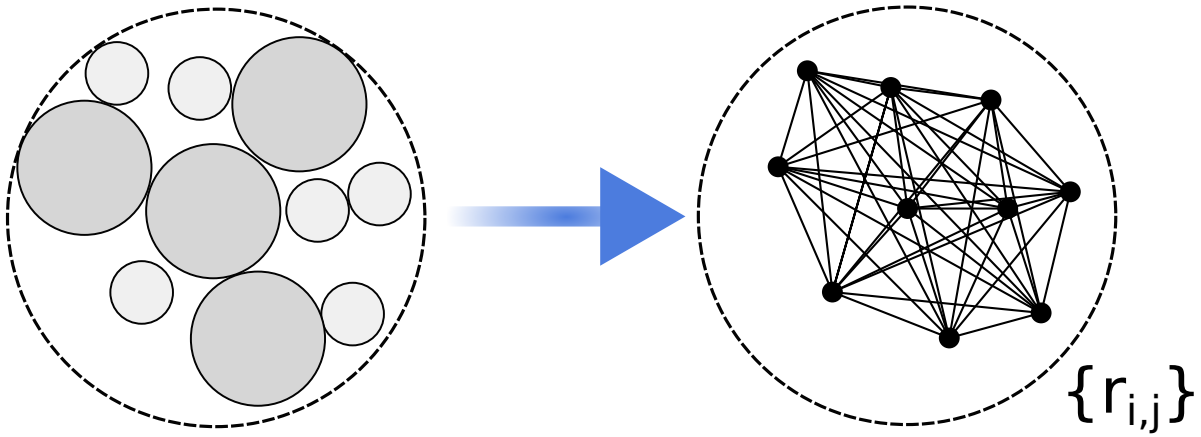

1. random agglomerate shape
2. initial structure of overlapping primary particles
3. collective rearrangement of primary particles
4. bond network
   - bond radii $r_{i,j}$: realizations of $K_{i,j} \cdot \min\{r_i, r_j\}$ for $i, j = 1, \ldots, n$, with $K_{i,j}$ independent and F_{K_b}-distributed

Stochastic modeling of the 3D microstructure

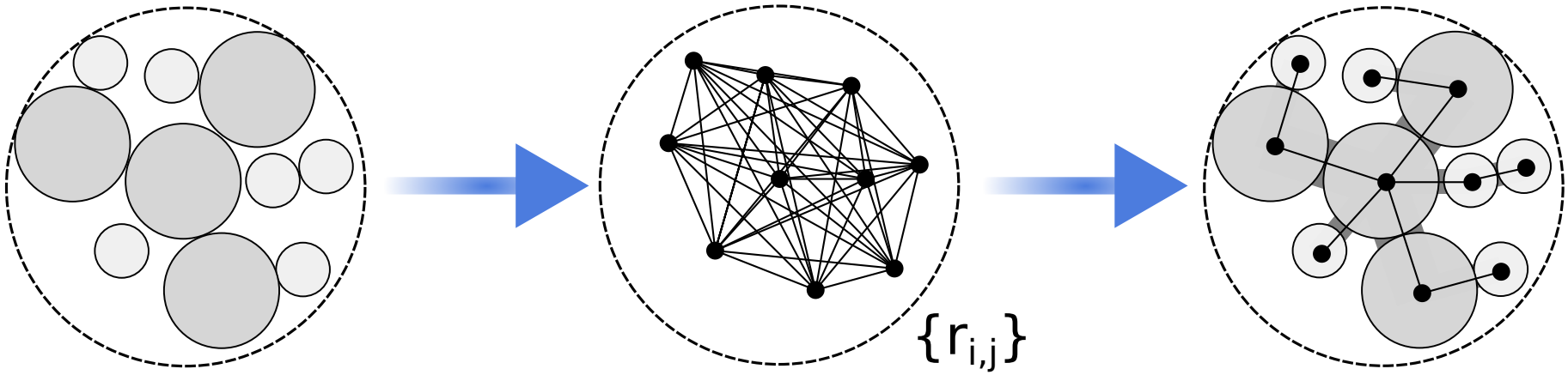

1. random agglomerate shape
2. initial structure of overlapping primary particles
3. collective rearrangement of primary particles
4. bond network
   - bond radii $r_{i,j}$: realizations of $K_{i,j} \cdot \min\{r_i, r_j\}$ for $i, j = 1, \ldots, n$, with $K_{i,j}$ independent and F_{K_b}-distributed
   - existence of bonds:
     - (relative) total bond volume b: realization of $\mathbb{B}$
     - particle distance threshold ℓ: approximate targeted total bond volume
     - minimum spanning tree to ensure connectivity

Stochastic modeling of the 3D microstructure

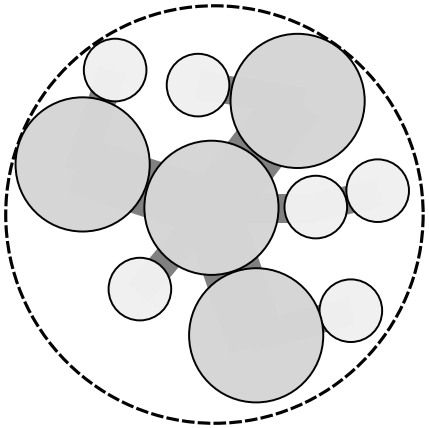

1. random agglomerate shape
2. initial structure of overlapping primary particles
3. collective rearrangement of primary particles
4. bond network

3D microstructure model: real maltodextrin agglomerates

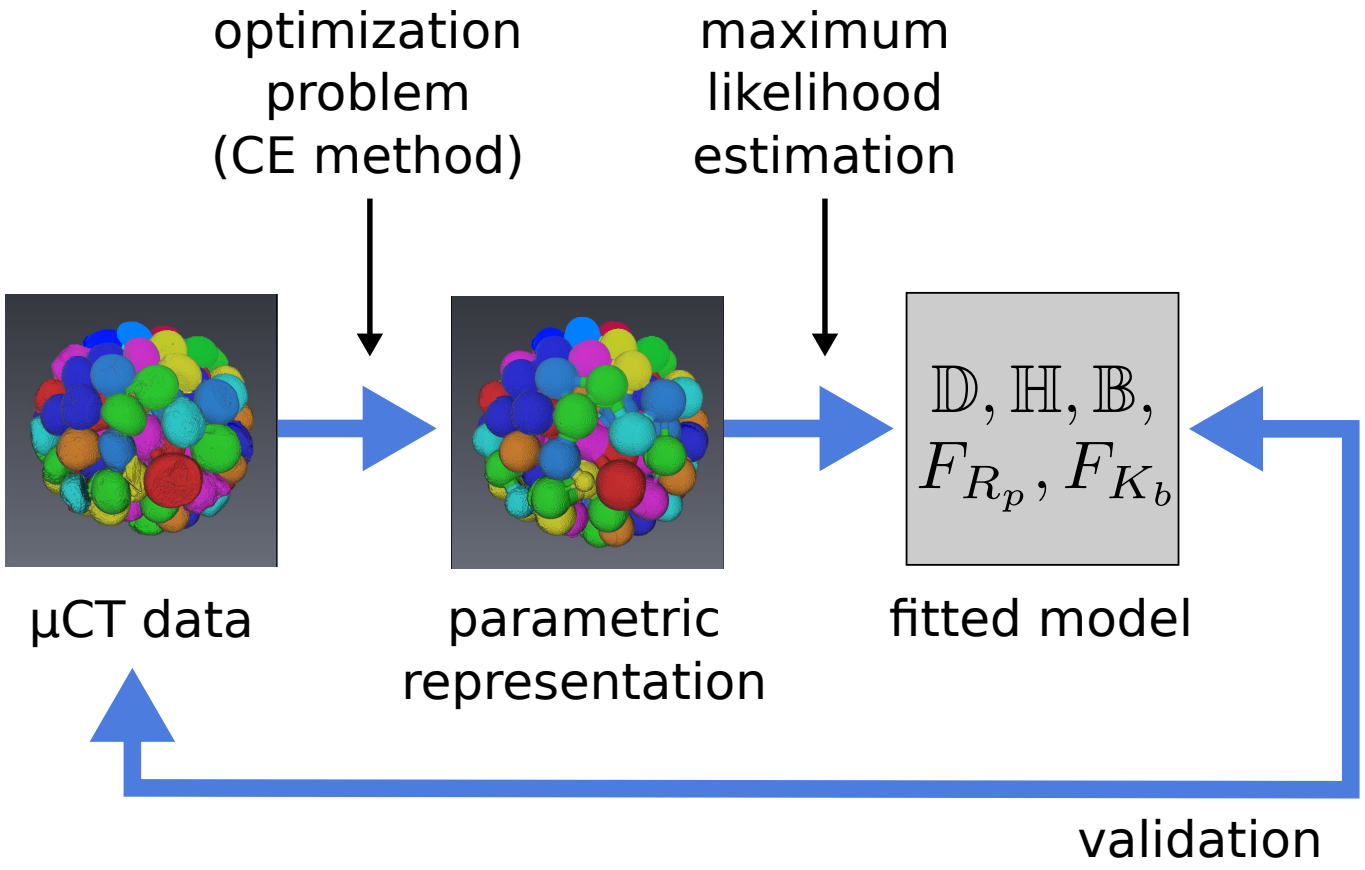

Conclusion

- model is suitable to describe real agglomerate structures

A. Spettl, S. Bachstein, M. Dosta, M. Goslinska, S. Heinrich and V. Schmidt, Bonded-particle extraction and stochastic modeling of internal agglomerate structures. *Advanced Powder Technology* 27 (2016), 1761–1774.

Numerical investigation of breakage behavior

Virtual experiment

- static loading: compression between two metal plates
- output:
  - time-resolved microstructure up to agglomerate breakage
  - force-displacement curve
- simulation method: discrete element method (DEM) with bonded-particle model (BPM)

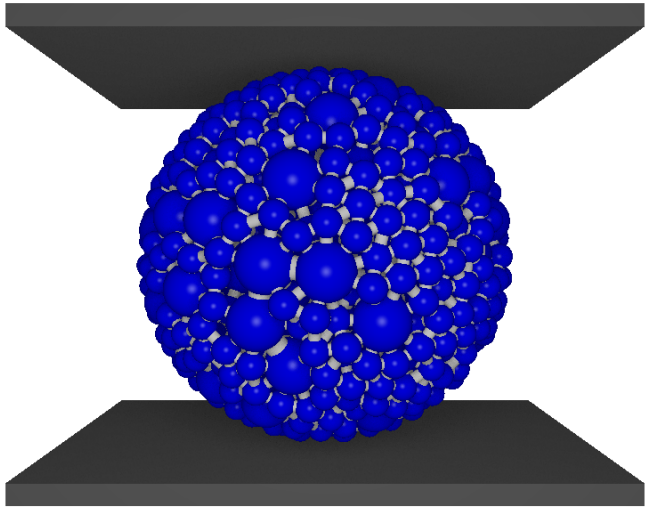

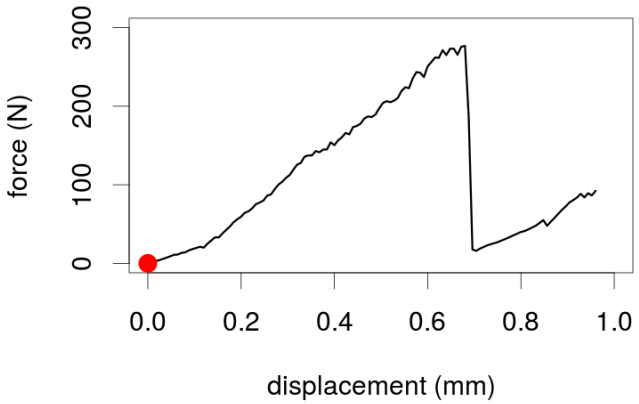

Numerical investigation of breakage behavior

Virtual experiment

- static loading: compression between two metal plates
- output:
  - time-resolved microstructure up to agglomerate breakage
  - force-displacement curve
- simulation method: discrete element method (DEM) with bonded-particle model (BPM)

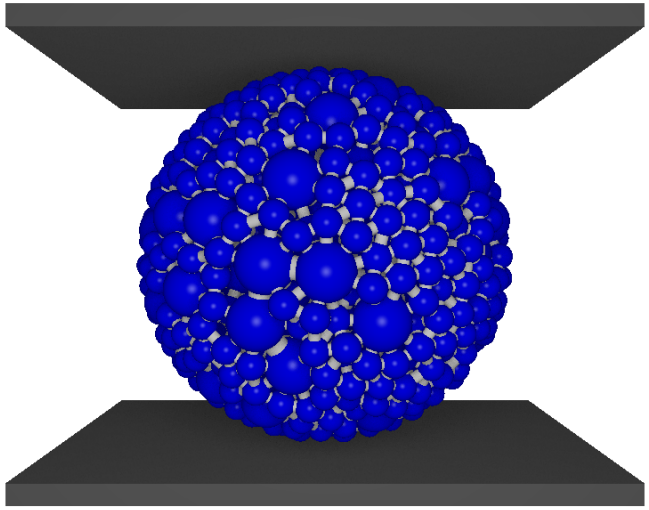

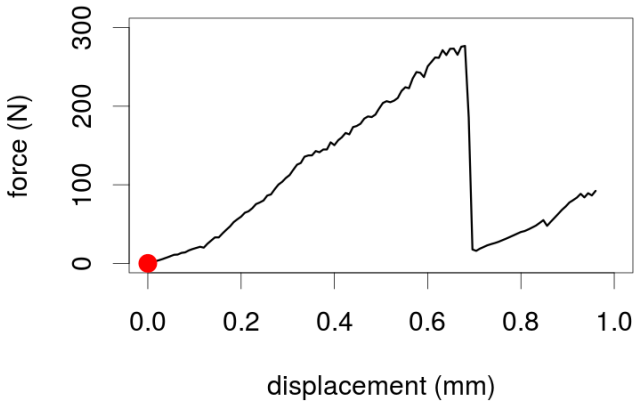

Prediction model for breakage behavior properties

input:
structural
properties

tailored
microstructures

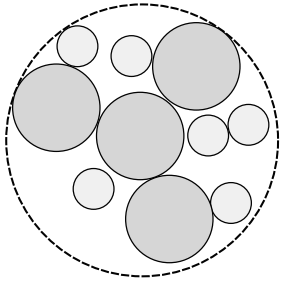

DEM simulation of
compression

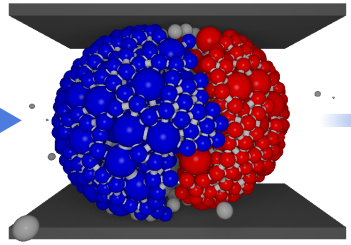

output:
- breakage energy
- fragment sizes

Prediction model for breakage behavior properties

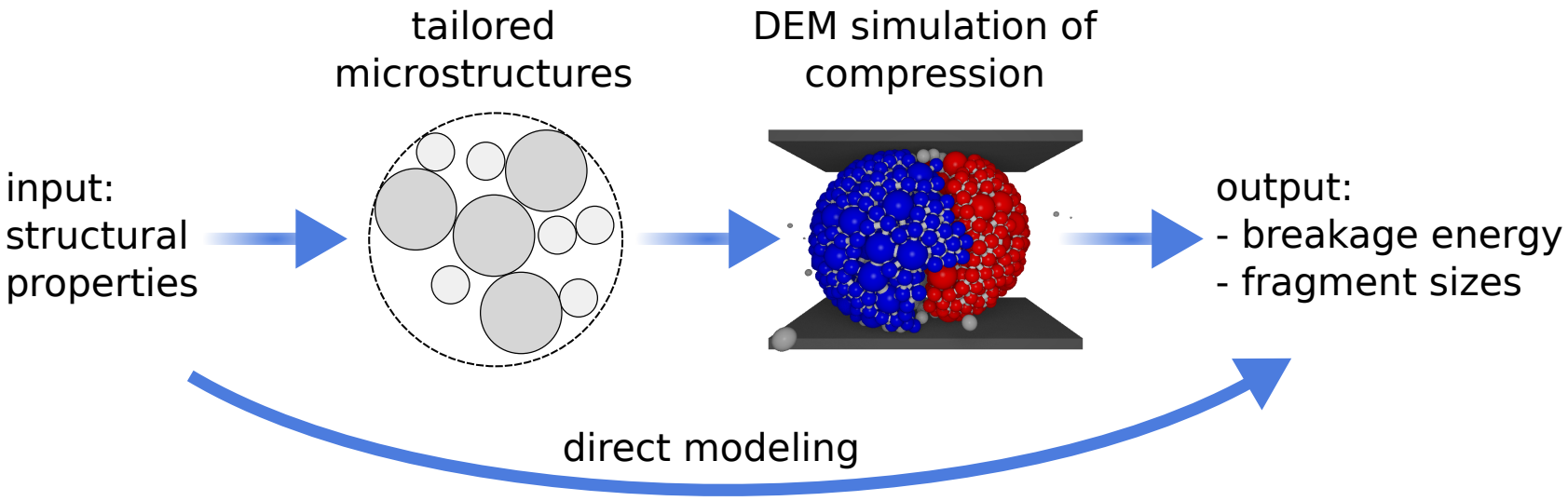

Aim: breakage probability and fragment sizes for a given stress energy

Prediction model for breakage behavior properties

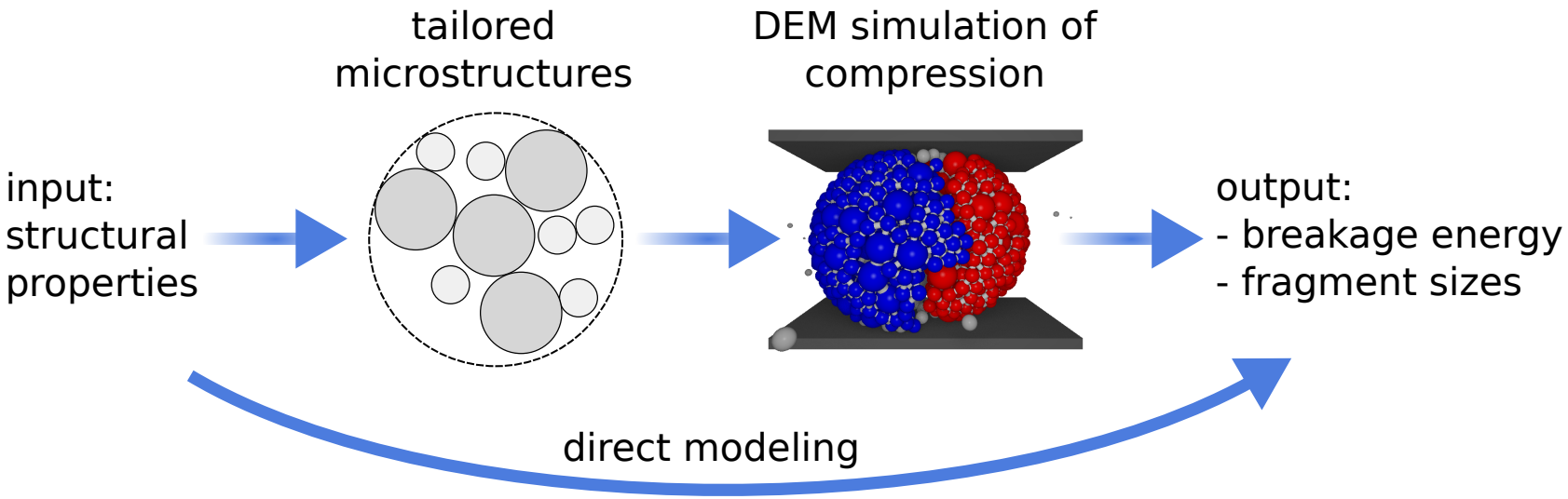

Aim: breakage probability and fragment sizes for a given stress energy

Random vector model

Example: agglomerate radius as independent variable

- breakage energies: (X_r, X_w)
- fragment sizes: $(\tilde{X}_r, X_m)$

Conditional distributions

For a fixed radius r and stress energy w

- breakage probability: $p_{\text{break}}(w) = \mathbb{P}(X_w \leq w \mid X_r = r)$
- fragment size distribution: $F_{\text{fragm}}(m) = \mathbb{P}(X_m \leq m \mid \tilde{X}_r = r)$

Prediction model for breakage behavior properties

Model choice and fitting

Data: e.g. simulation results of 1000 agglomerates yield:

- breakage energies: $(x_r^{(i)}, x_w^{(i)})$, $i = 1, \ldots, 1000$
- fragment sizes: $(x_r^{(i)}, x_m^{(i,j)})$, $i = 1, \ldots, 1000$, $j = 1, \ldots, n(i)$

$\Rightarrow$ interpretation as samples of random vectors (X_r, X_w) and $(\tilde{X}_r, X_m)$, use copula-based distributions

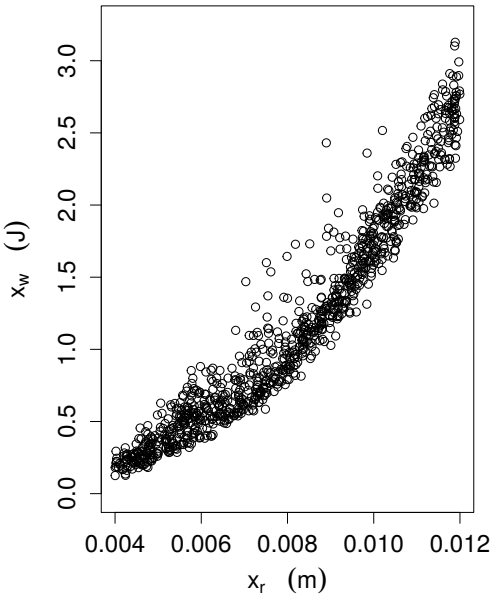

simulation results $(x_r^{(i)}, x_w^{(i)})$

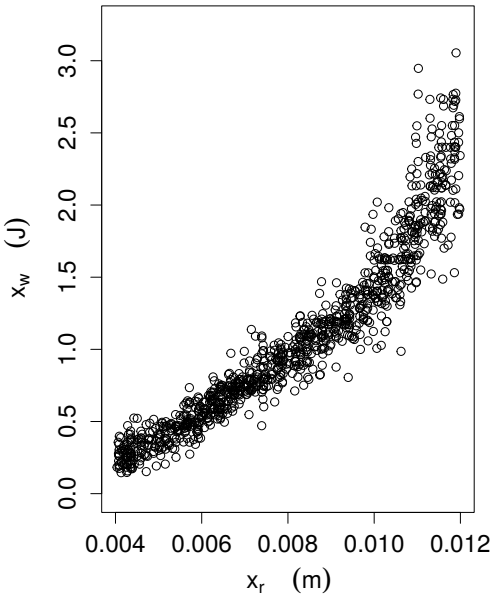

realizations of (X_r, X_w)

Grain coarsening in polycrystalline materials

Real data

Time-resolved 3D data of Al–Cu sample during heat treatment:
Ostwald ripening at ultra-high volume fraction of the coarsening phase

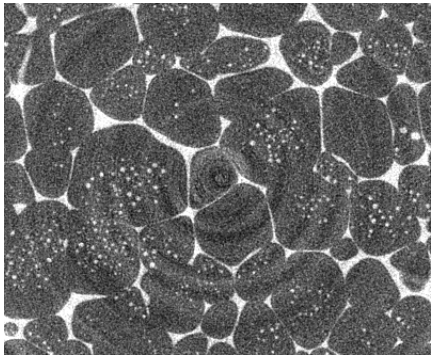

initial time

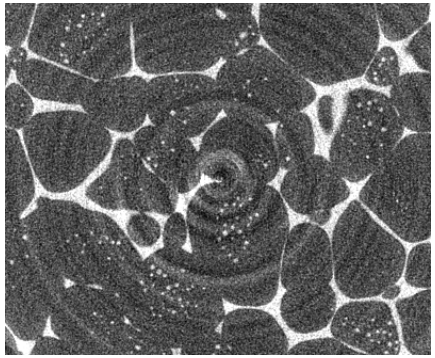

+400 minutes

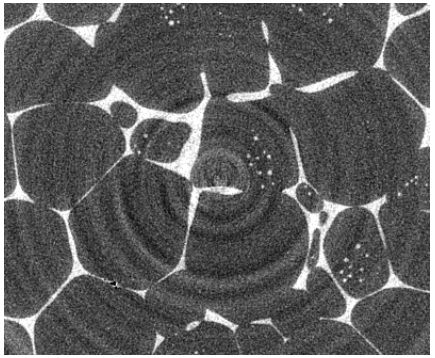

+800 minutes

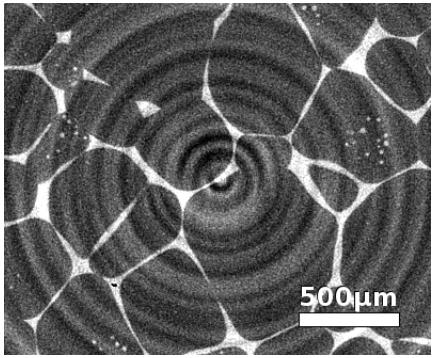

+1200 minutes

Grain coarsening in polycrystalline materials

Real data

Time-resolved 3D data of Al–Cu sample during heat treatment:
Ostwald ripening at ultra-high volume fraction of the coarsening phase

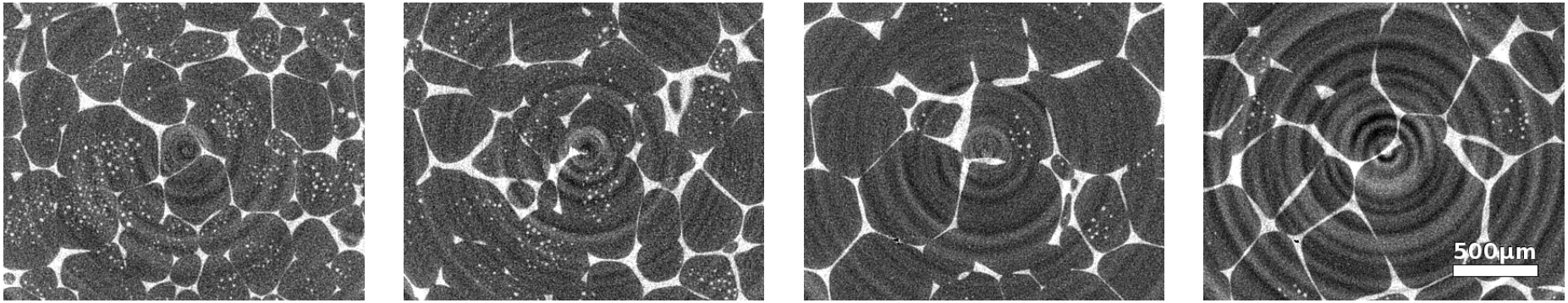

initial time | +400 minutes | +800 minutes | +1200 minutes

Properties in the steady state of the sample

Let R_t denote the typical (volume-equivalent) grain radius at time $t \geq 0$ and $\bar{R}_t = \mathbb{E}R_t$. For $t > 0$ it holds:

- power-law growth: $\bar{R}_t^3 - \bar{R}_0^3 = kt$ with $k > 0$
- self-similarity: $R_t/\bar{R}_t \stackrel{\mathrm{D}}{=} R_0/\bar{R}_0$

Stochastic modeling of the 3D microstructure

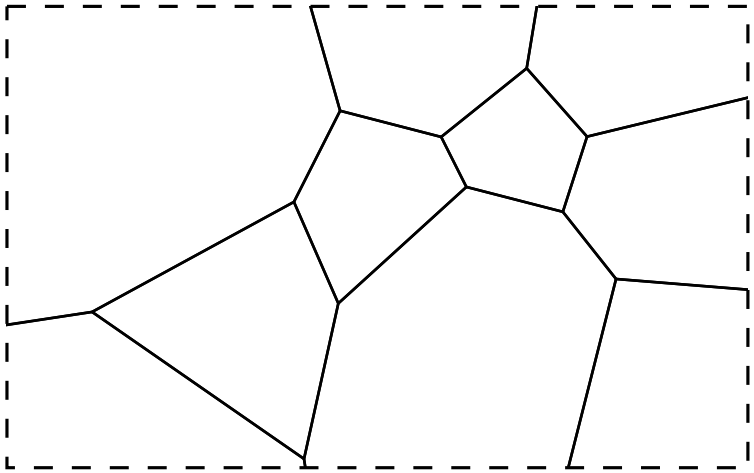

1. marked point process
2. "hard cores" for marked points
3. Laguerre tessellation
4. linking time t to model parameters

A. Spettl, R. Wimmer, T. Werz, M. Heinze, S. Odenbach, C. E. Krill III and V. Schmidt, Stochastic 3D modeling of Ostwald ripening at ultra-high volume fractions of the coarsening phase. *Modelling and Simulation in Materials Science and Engineering* 23 (2015), 065001.

Stochastic modeling of the 3D microstructure

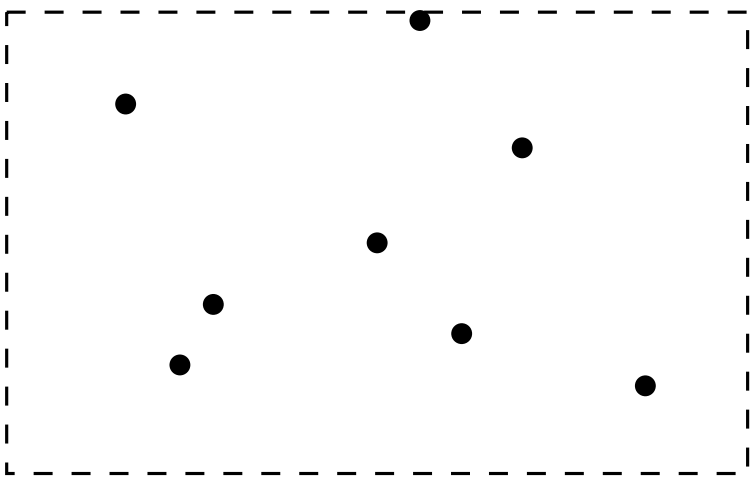

1. marked point process
   - homogeneous Poisson point process $\{S_i\}_{i\in\mathbb{N}}$ with intensity λ
2. "hard cores" for marked points
3. Laguerre tessellation
4. linking time t to model parameters

Stochastic modeling of the 3D microstructure

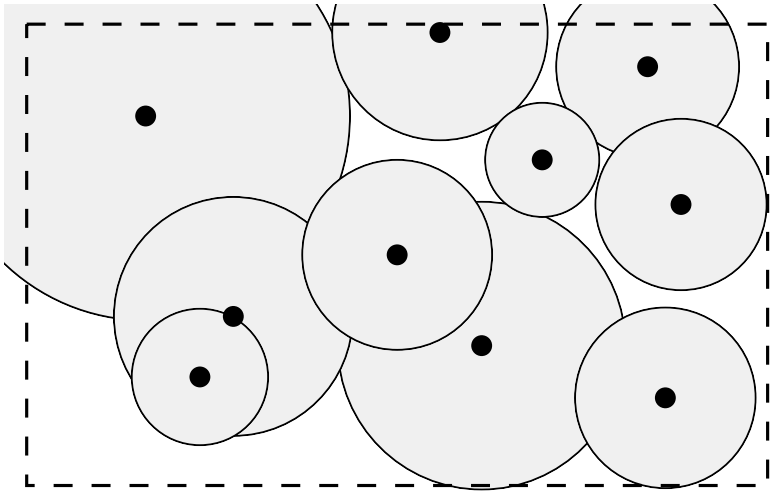

1. marked point process
   - homogeneous Poisson point process $\{S_i\}_{i\in\mathbb{N}}$ with intensity λ
   - independent marks $\{R_i\}_{i\in\mathbb{N}}$, $R_i \sim \mathcal{N}_+(\mu, \sigma^2)$
   - λ is fixed by (scale independent) parameter $\eta = \lambda \frac{4}{3}\pi\mathbb{E}(R_1^3)$
2. "hard cores" for marked points
3. Laguerre tessellation
4. linking time t to model parameters

Stochastic modeling of the 3D microstructure

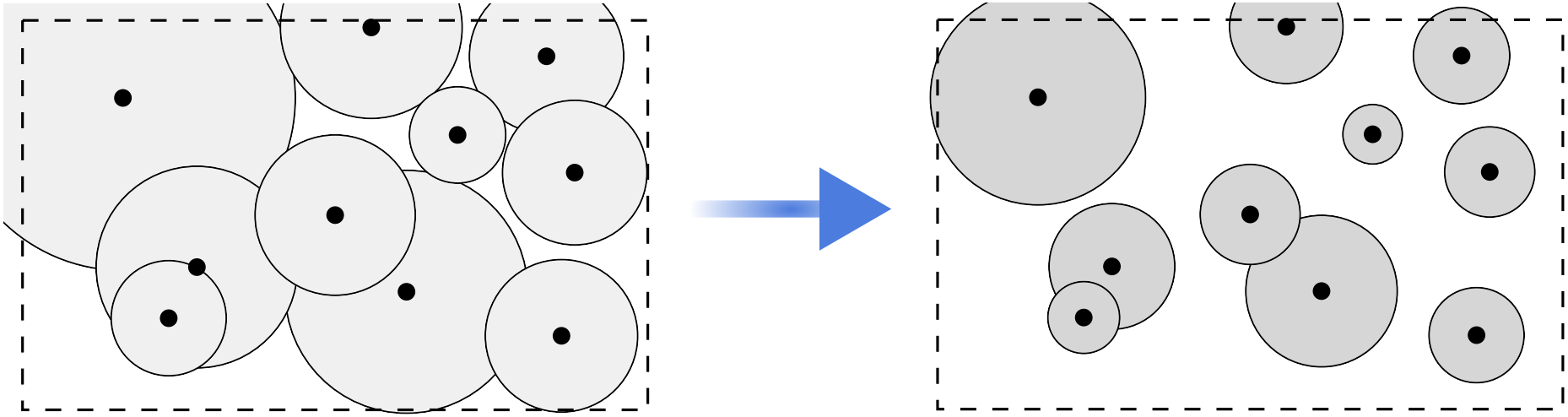

1. marked point process
2. "hard cores" for marked points
   - for $\tau \in (0, 1]$, define a hard core $(S_i, \tau R_i)$ for every marked point
3. Laguerre tessellation
4. linking time t to model parameters

Stochastic modeling of the 3D microstructure

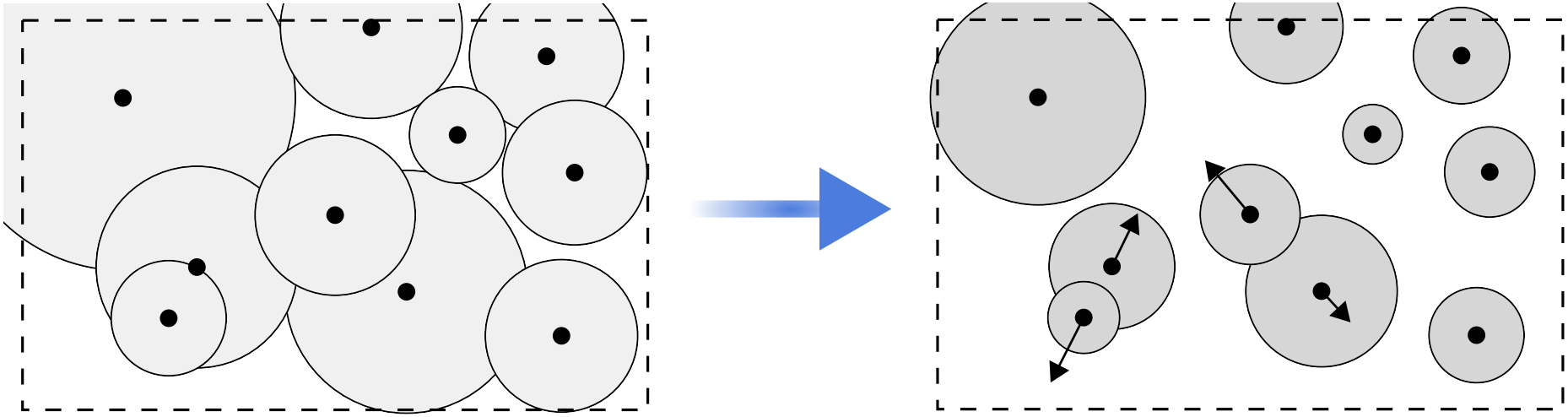

1. marked point process
2. "hard cores" for marked points
   - for $\tau \in (0, 1]$, define a hard core $(S_i, \tau R_i)$ for every marked point
   - collective rearrangement to avoid overlapping
3. Laguerre tessellation
4. linking time t to model parameters

Stochastic modeling of the 3D microstructure

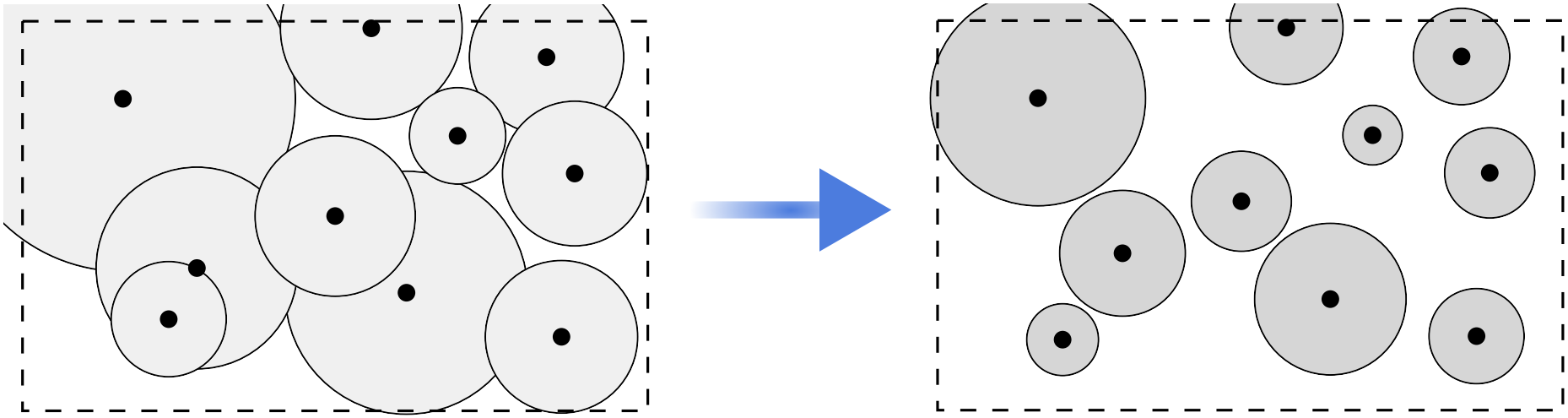

1. marked point process
2. "hard cores" for marked points
   - for $\tau \in (0, 1]$, define a hard core $(S_i, \tau R_i)$ for every marked point
   - collective rearrangement to avoid overlapping
3. Laguerre tessellation
4. linking time t to model parameters

Stochastic modeling of the 3D microstructure

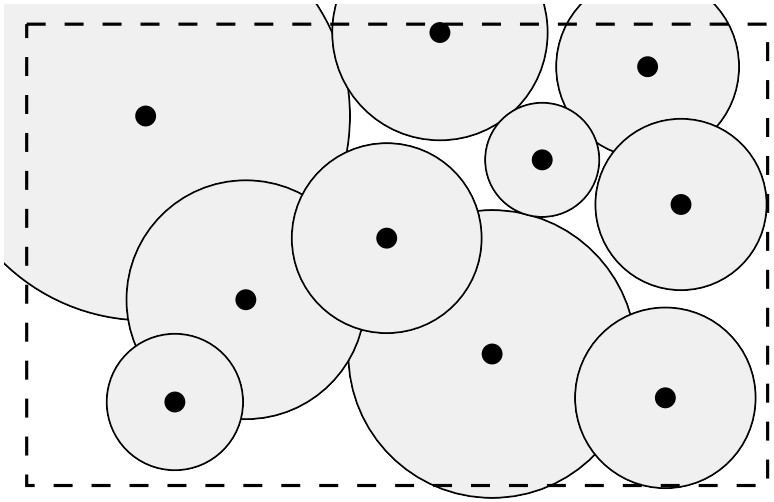

1. marked point process
2. "hard cores" for marked points
3. Laguerre tessellation
4. linking time t to model parameters

Stochastic modeling of the 3D microstructure

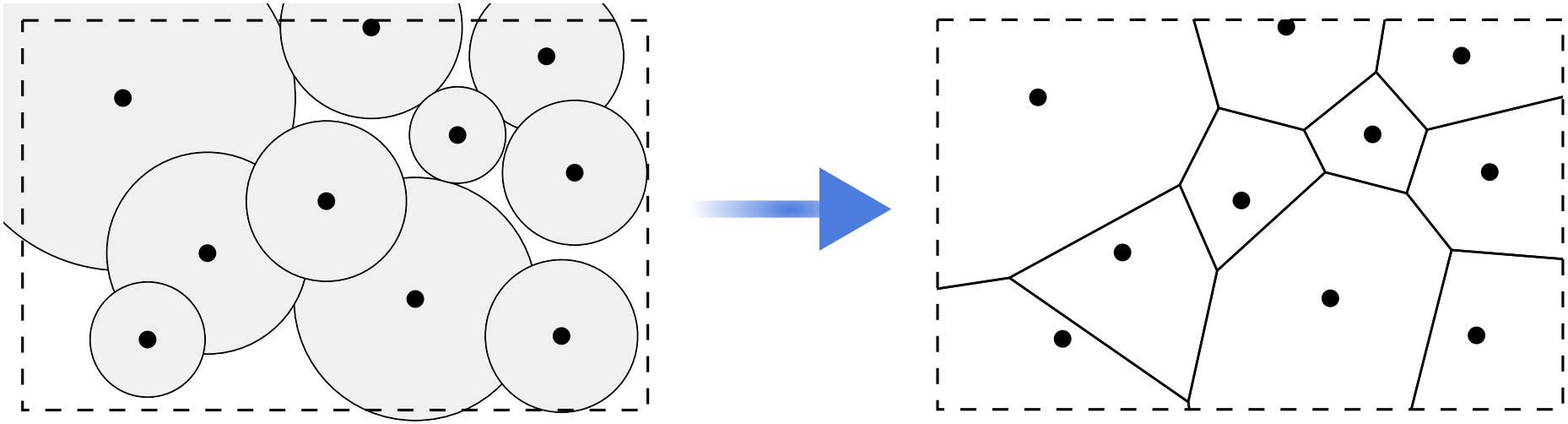

1. marked point process
2. "hard cores" for marked points
3. Laguerre tessellation
   - Laguerre cell C_i for each marked point (S_i, R_i)

$$C_i = \{x \in \mathbb{R}^3 : \|x - S_i\|^2 - R_i^2 \leq \|x - S_j\|^2 - R_j^2 \text{ for all } j \in \mathbb{N}\}$$

   - non-empty Laguerre cells form the Laguerre tessellation
4. linking time t to model parameters

Stochastic modeling of the 3D microstructure

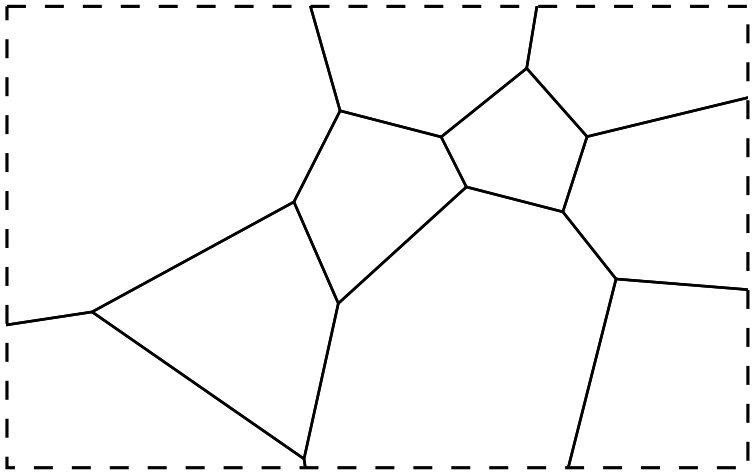

1. marked point process
2. "hard cores" for marked points
3. Laguerre tessellation
   - Laguerre cell C_i for each marked point (S_i, R_i)

$$C_i = \{x \in \mathbb{R}^3 : \|x - S_i\|^2 - R_i^2 \leq \|x - S_j\|^2 - R_j^2 \text{ for all } j \in \mathbb{N}\}$$

   - non-empty Laguerre cells form the Laguerre tessellation
4. linking time t to model parameters

Stochastic modeling of the 3D microstructure

$$\begin{pmatrix} \mu \\ \sigma^2 \\ \tau \\ \eta \end{pmatrix} = p(t) = \begin{pmatrix} c_\mu \bar{R}_t \\ \left(c_\sigma \bar{R}_t\right)^2 \\ \tau \\ \eta \end{pmatrix} \quad \text{with} \quad \bar{R}_t = \sqrt[3]{\bar{R}_0^3 + kt}$$

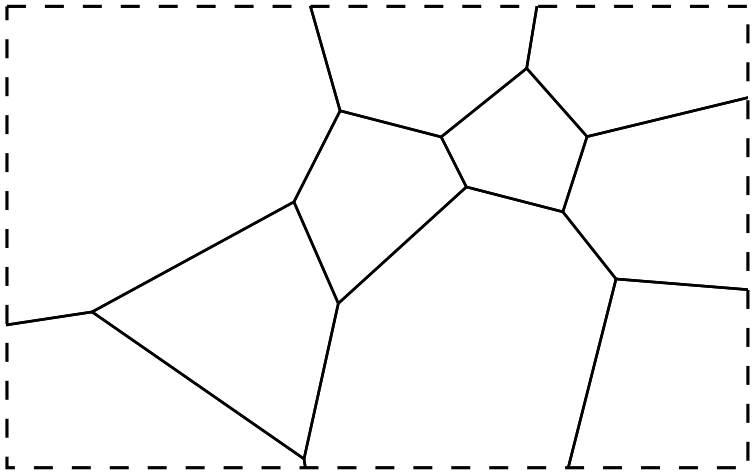

1. marked point process
2. "hard cores" for marked points
3. Laguerre tessellation
4. linking time t to model parameters
   - express parameters μ, σ, τ, η as a function of t
   - by construction: power-law growth and self-similarity

Stochastic modeling of the 3D microstructure

Parameter estimation

- power-law growth: least-squares fit to determine k and $\bar{R}_0$

$$\begin{pmatrix} \widehat{k} \\ \widehat{\bar{R}}_0 \end{pmatrix} = \underset{(k,\bar{R}_0)\in\mathbb{R}_+\times\mathbb{R}_+}{\arg\min} \sum_{t\in T_{\exp}} \left(\widehat{\bar{R}}_t - \sqrt[3]{\bar{R}_0^3 + kt} \right)^2$$

- remaining parameters: minimum-contrast estimation

$$\begin{pmatrix} \widehat{c_\mu} \\ \widehat{c_\sigma} \\ \widehat{\tau} \\ \widehat{\eta} \end{pmatrix} = \underset{(c_\mu,c_\sigma,\tau,\eta)\in\Psi}{\arg\min} \sum_{t\in T_{\exp}} \int_0^\infty \left(\widehat{F}_R^{(t)}(r) - F_R^{(t)}(r) \right)^2 \mathrm{d}r$$

Stochastic modeling of the 3D microstructure

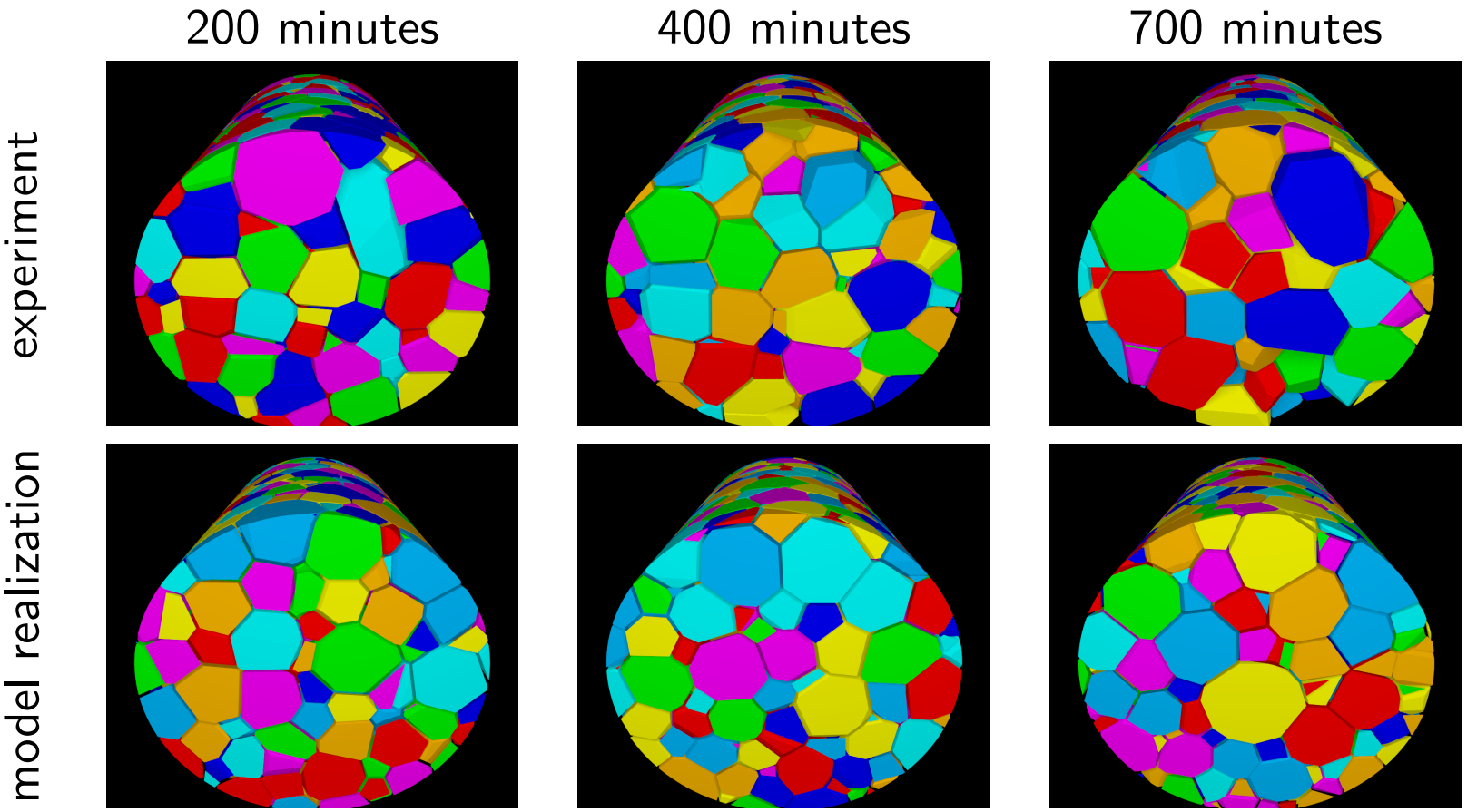

Markov chain for the evolution of grain radii

Aim and approach

- stochastic process $\{\mathring{R}_t\}_{t\in T}$ that describes the radius evolution of the typical grain
- choose $\mathring{R}_0 = R_0$ and T discrete with $T = \{0, t_{\text{step}}, 2t_{\text{step}}, \ldots\}$
- Markov assumption $\Rightarrow$ (time-dependent) transition kernel needed:

$$P_t(r, A) = \mathbb{P}(\mathring{R}_{t+t_{\text{step}}} \in A \mid \mathring{R}_t = r), \quad t \in T$$

A. Spettl, T. Werz, C. E. Krill III and V. Schmidt, Stochastic modeling of individual grain behavior during Ostwald ripening at ultra-high volume fractions of the coarsening phase. *Computational Materials Science* 124 (2016), 290–303.

Markov chain for the evolution of grain radii

Aim and approach

- stochastic process $\{\mathring{R}_t\}_{t\in T}$ that describes the radius evolution of the typical grain
- choose $\mathring{R}_0 = R_0$ and T discrete with $T = \{0, t_{\text{step}}, 2t_{\text{step}}, \ldots\}$
- Markov assumption $\Rightarrow$ (time-dependent) transition kernel needed:

$$P_t(r, A) = \mathbb{P}(\mathring{R}_{t+t_{\text{step}}} \in A \mid \mathring{R}_t = r), \quad t \in T$$

Known information

- distribution function F_{R_t} of R_t (power-law growth and self-similarity)
- $F_{\mathring{R}_t}(x) = (1 - q_t)F_{R_t}(x) + q_t \mathbb{1}_{[0,\infty)}(x)$ with $q_t = 1 - \bar{R}_0^3/\bar{R}_t^3$

Markov chain for the evolution of grain radii

Aim and approach

- stochastic process $\{\mathring{R}_t\}_{t\in T}$ that describes the radius evolution of the typical grain
- choose $\mathring{R}_0 = R_0$ and T discrete with $T = \{0, t_{\text{step}}, 2t_{\text{step}}, \ldots\}$
- Markov assumption $\Rightarrow$ (time-dependent) transition kernel needed:

$$P_t(r, A) = \mathbb{P}(\mathring{R}_{t+t_{\text{step}}} \in A \mid \mathring{R}_t = r), \quad t \in T$$

Known information

- distribution function F_{R_t} of R_t (power-law growth and self-similarity)
- $F_{\mathring{R}_t}(x) = (1 - q_t)F_{R_t}(x) + q_t \mathbb{1}_{[0,\infty)}(x)$ with $q_t = 1 - \bar{R}_0^3/\bar{R}_t^3$

Missing information

- joint distribution of $(\mathring{R}_t, \mathring{R}_{t+t_{\text{step}}})$ for $t \in T$

Choice of copula

Requirement: absorbing state

- $\mathbb{P}(\mathring{R}_{t+t_{\text{step}}} = 0 \mid \mathring{R}_t = 0) = 1$

Choice of copula

Requirement: absorbing state

- $\mathbb{P}(\mathring{R}_{t+t_{\text{step}}} = 0 \mid \mathring{R}_t = 0) = 1$

co-monotonicity copula	Gauß copula	vine copula
deterministic global growth behavior	ordinal sum construction with 2 components random walk (with global growth behavior)	extension of state space integration of local characteristics (e. g. mean grain radius of neighborhood)

Experimental and simulated trajectories

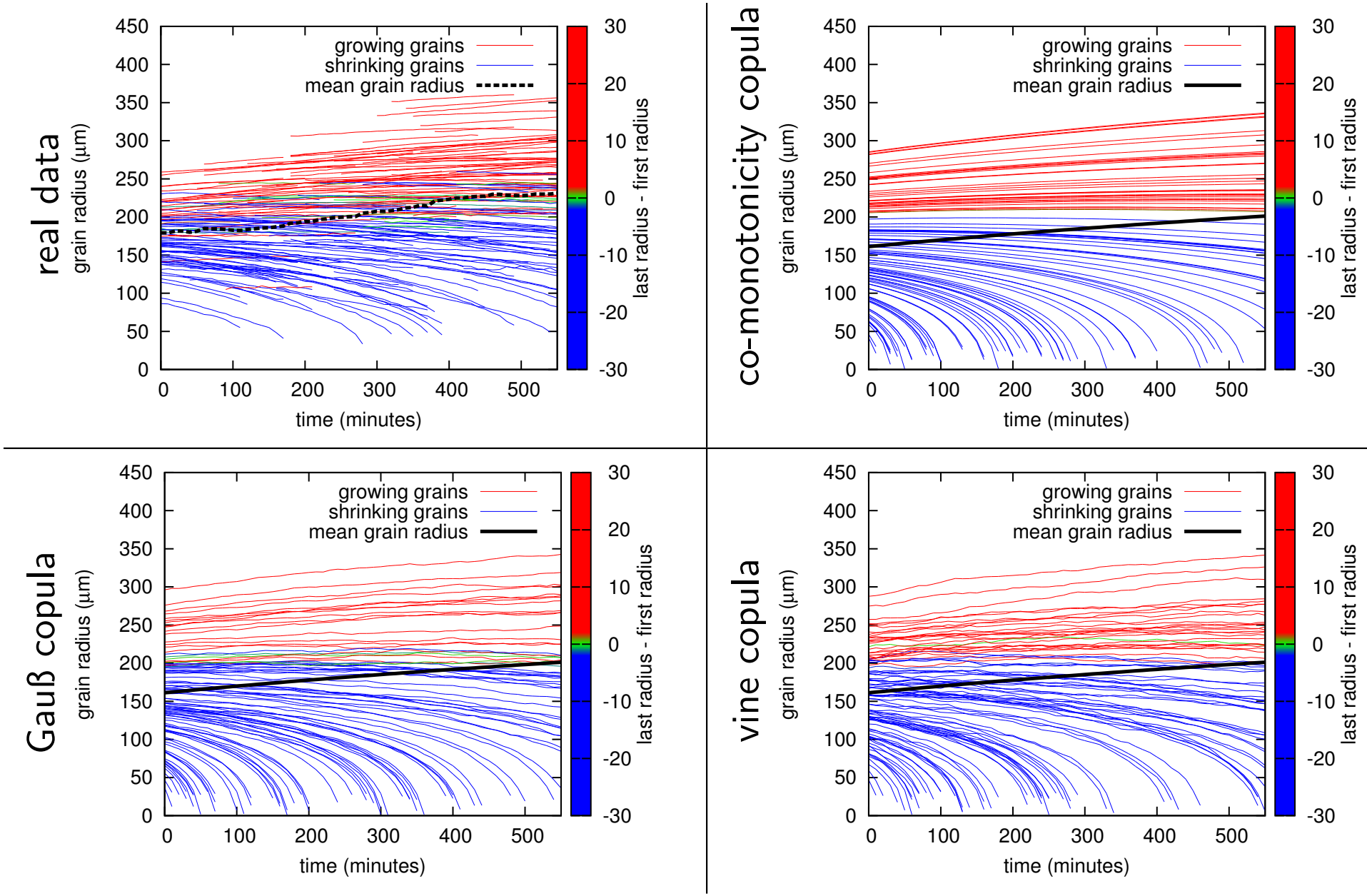

Simulation of Ostwald ripening in 3D

Visualization

- combination of stochastic 3D model and Markov chain model

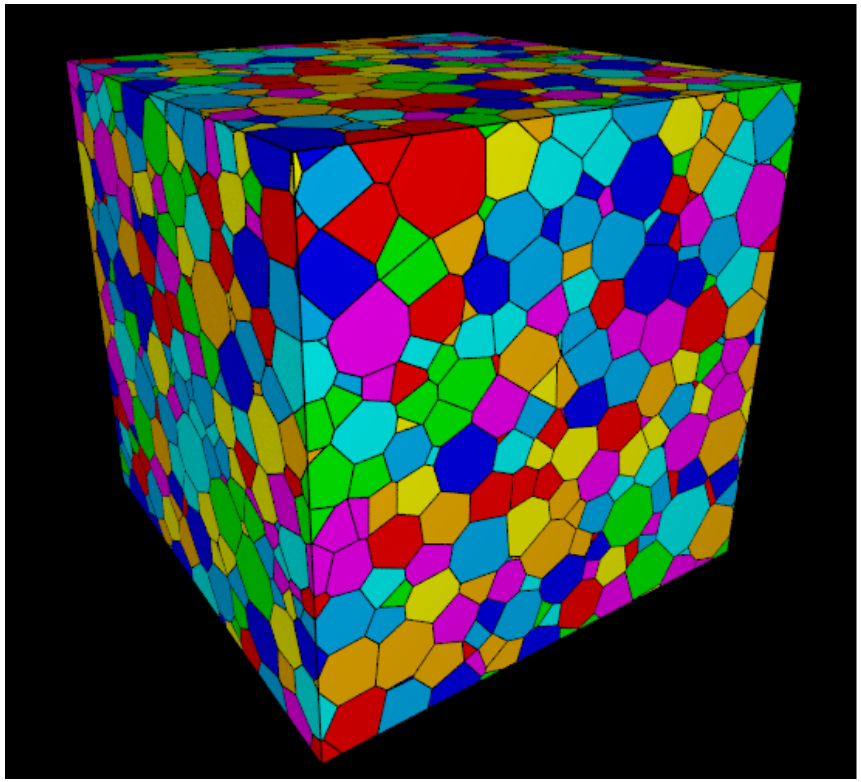

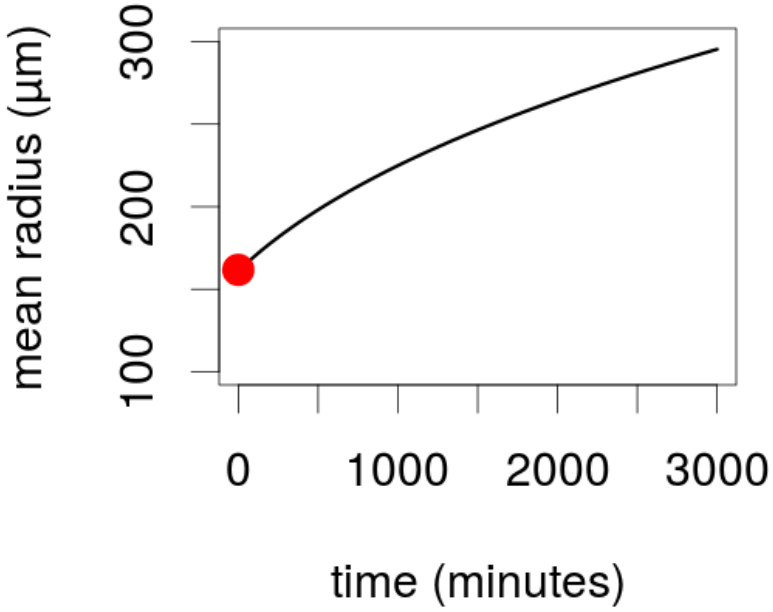

Simulation of Ostwald ripening in 3D

Visualization

- combination of stochastic 3D model and Markov chain model

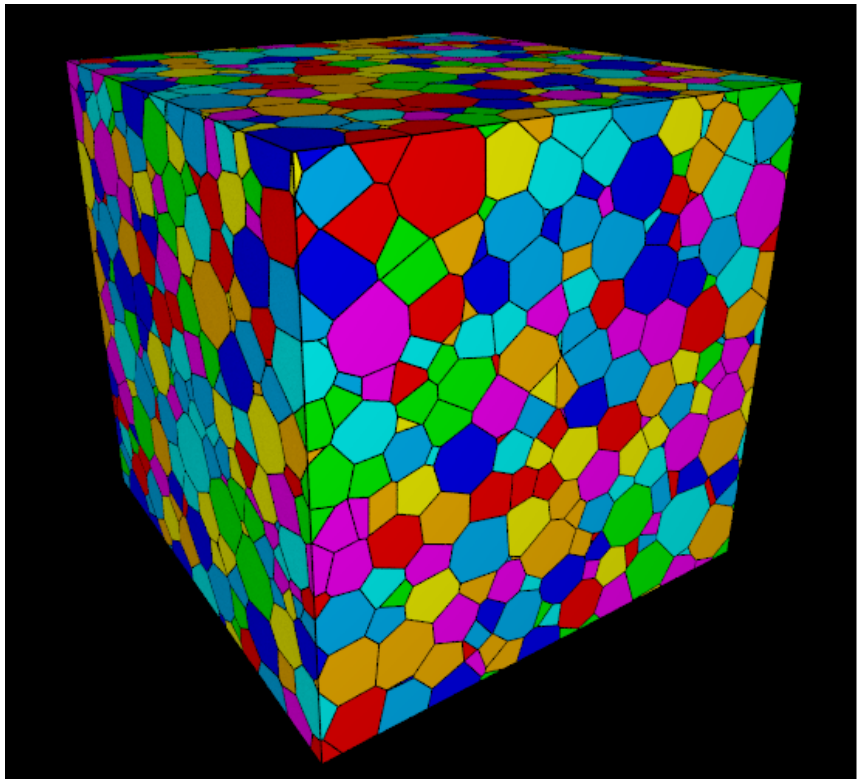

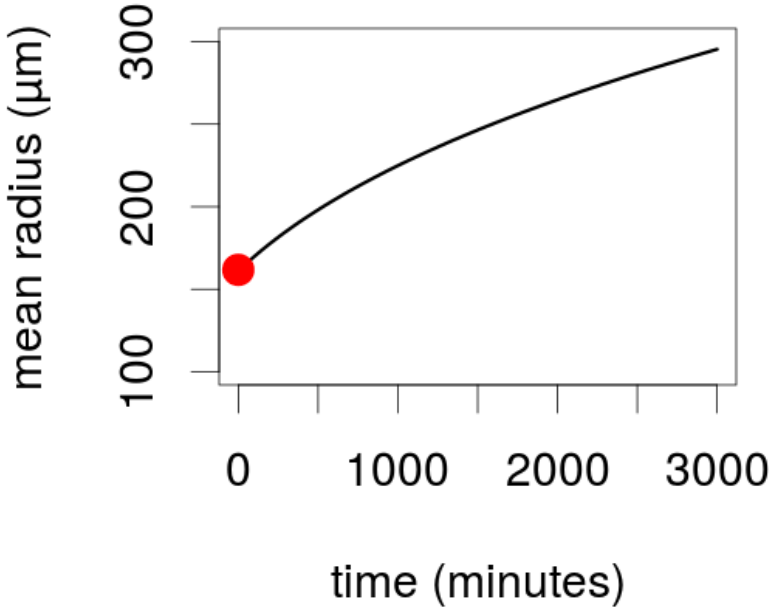

Further results

Problem

- parametric description of cells for unknown Laguerre generator points
- Laguerre inversion for perfect data
- Laguerre approximation for discrete and/or noisy data

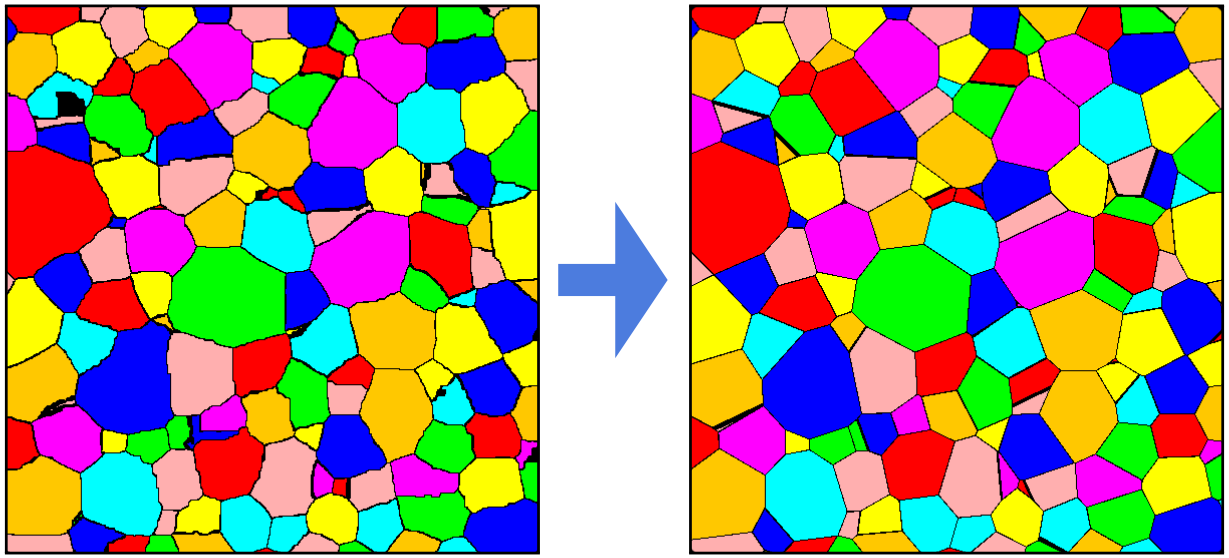

segmentation of real data Laguerre approximation

A. Spettl, T. Werz, C. E. Krill III and V. Schmidt, Parametric representation of 3D grain ensembles in polycrystalline microstructures. *Journal of Statistical Physics* 154 (2014), 913–928.
A. Spettl, T. Brereton, Q. Duan, T. Werz, C. E. Krill III, D. P. Kroese and V. Schmidt, Fitting Laguerre tessellation approximations to tomographic image data. *Philosophical Magazine* 96 (2016), 166–189.

J. Feinauer, A. Spettl, I. Manke, S. Strege, A. Kwade, A. Pott and V. Schmidt, Structural characterization of particle systems using spherical harmonics. *Materials Characterization* 106 (2015), 123-133.

J. Feinauer, T. Brereton, A. Spettl, M. Weber, I. Manke and V. Schmidt, Stochastic 3D modeling of the microstructure of lithium-ion battery anodes via Gaussian random fields on the sphere. *Computational Materials Science* 109 (2015), 137-146.

S. Hein, J. Feinauer, D. Westhoff, I. Manke, V. Schmidt and A. Latz, Stochastic microstructure modelling and electrochemical simulation of lithium-ion cell anodes in 3D. *Journal of Power Souces* (submitted).

D. Westhoff, J. Feinauer, K. Kuchler, T. Mitsch, I. Manke, S. Hein, A. Latz and V. Schmidt, Parametric stochastic 3D model for the microstructure of anodes in lithium-ion power cells. *Computational Materials Science* (under revision).

A. Spettl, M. Dosta, S. Antonyuk, S. Heinrich and V. Schmidt, Statistical investigation of agglomerate breakage based on combined stochastic microstructure modeling and DEM simulations. *Advanced Powder Technology* 26 (2015), 1021–1030.

A. Spettl, S. Bachstein, M. Dosta, M. Goslinska, S. Heinrich and V. Schmidt, Bonded-particle extraction and stochastic modeling of internal agglomerate structures. *Advanced Powder Technology* 27 (2016), 1761-1774.

A. Spettl, R. Wimmer, T. Werz, M. Heinze, S. Odenbach, C. E. Krill III and V. Schmidt, Stochastic 3D modeling of Ostwald ripening at ultra-high volume fractions of the coarsening phase. *Modelling and Simulation in Materials Science and Engineering* 23 (2015), 065001.

A. Spettl, T. Werz, C. E. Krill III and V. Schmidt, Stochastic modeling of individual grain behavior during Ostwald ripening at ultra-high volume fractions of the coarsening phase. *Computational Materials Science* 124 (2016), 290-303.

A. Spettl, T. Werz, C. E. Krill III and V. Schmidt, Parametric representation of 3D grain ensembles in polycrystalline microstructures. *Journal of Statistical Physics* 154 (2014), 913–928.

A. Spettl, T. Brereton, Q. Duan, T. Werz, C. E. Krill III, D. P. Kroese and V. Schmidt, Fitting Laguerre tessellation approximations to tomographic image data. *Philosophical Magazine* 96 (2016), 166–189.